Summer 2002

Masseter muscle activity resulting from stimulation of hypothalamic behavioral sites : wavelet analysis

Anne Marie Petrock
New Jersey Institute of Technology

ABSTRACT

MASSETER MUSCLE ACTIVITY RESULTING FROM STIMULATION OF HYPOTHALAMIC BEHAVIORAL SITES: A WAVELET ANALYSIS

by
Anne Marie Petrock

Patterns of electromyographic (EMG) activity can give an insight into muscle activity associated with a given behavioral state. The masseter muscle is positioned closely to the temporomandibular joint and controls the position and movement of the jaw. The hypothalamus is the region of the brain associated with emotional behavior. In an effort to further understand the muscle activity underlying emotional display, the hypothalamus in two cats was stimulated to evoke a stereotyped emotional response, known as the "rage response." Unsheathing of the claws, retraction of the ears, significant pupillary dilation and vocalization (hissing) characterize this behavior. EMG data obtained at the masseter muscle during this emotional state were compared to EMG activity recorded during mastication (eating), the simulated voluntary behavior for this study.

The results of this study indicate that the emotional state significantly influences the EMG activity in the masseter muscle. This is evidenced statistically by a larger high frequency component in the EMG data. It is also evidenced by the ratio of stimulation to mastication power levels at different frequencies, which increases as frequency increases.

The frequency range between 5-30 Hz has been utilized in the past in studies assessing fatigue. However, the results of this research indicate that the interpretation of the data in this frequency band must be different in studies of emotionally elicited muscle response. Recordings obtained during voluntary muscular activity reflected the typical fatigue response, and appropriate elevations in the power in the 5-30 Hz frequency range occurred, in agreement with previous findings. Recordings obtained during stimulation indicate that the highest power in this frequency band is achieved at the onset of hypothalamic stimulation, rather than at the point in time when fatigue typically occurs, in contrast to previous findings.

MASSETER MUSCLE ACTIVITY RESULTING FROM STIMULATION OF HYPOTHALAMIC BEHAVIORAL SITES: A WAVELET ANALYSIS

by
Anne Marie Petrock

A Thesis
Submitted to the Faculty of
New Jersey Institute of Technology
In Partial Fulfillment of the Requirements for the Degree of
Masters of Science in Biomedical Engineering

Department of Biomedical Engineering

August 2002

APPROVAL PAGE

MASSETER MUSCLE ACTIVITY RESULTING FROM STIMULATION OF HYPOTHALAMIC BEHAVIORAL SITES: A WAVELET ANALYSIS

Anne Marie Petrock

Dr. Stanley S. Reisman, Thesis Advisor — Date
Professor of Biomedical Engineering, NJIT
Professor of Electrical and Computer Engineering, NJIT

Dr. Tara Alvarez, Committee Member — Date
Assistant Professor of Biomedical Engineering, NJIT

Dr. Saul Weiner, Committee Member — Date
Professor of Prosthodontics and Biomaterials, UMDNJ

BIOGRAPHICAL SKETCH

Author: Anne Marie Petrock

Degree: Master of Science

Date: August 2002

Undergraduate and Graduate Education:

- Master of Science in Biomedical Engineering
  New Jersey Institute of Technology, Newark, NJ, 2002.

- Bachelor of Science in Electrical Engineering
  New Jersey Institute of Technology, Newark, NJ, 1999

Major: Biomedical Engineering

Presentations and Publications:

Petrock, A., Reisman, S., Weiner, S., and A. Siegel, "Wavelet Analysis of Masseter Muscle Activity Resulting from Stimulation of Hypothalamic Behavioral Sites," *Proceedings of the 28th IEEE Annual Northeast Bioengineering Conference*, 2002, Drexel University, Philadelphia, Pennsylvania.

This thesis is dedicated to

my father, mother, Charlie and Chris, my biggest fans, who supported me with amazing patience and grace, and who never cease making me smile

and

my family and friends, both near and far, who never stopped believing in me.

ACKNOWLEDGMENT

The author would like to attempt to express her gratitude, which is beyond words, to her advisor, Dr. Stanley Reisman. He provided knowledge and encouragement that far exceeded his obligation. His patient guidance, subtle suggestions and unwavering support were the cornerstone upon which this thesis was constructed.

Special gratitude and appreciation are extended to Drs. Tara L. Alvarez and Saul K. Weiner for their collaboration as members of the thesis committee. Dr. Alvarez' encouragement and discussion of ideas was very beneficial to the completion of this research. Dr. Weiner gracefully provided the idea, data and much valuable medical information for this research. He also provided encouragement and freedom to explore new methods of signal processing. His patience and support throughout this research have been invaluable.

The author wishes to thank the New Jersey Commission on Higher Education, who provided financial support for this research.

Gratitude is extended to Ms. Gonzalez at the Office of Graduate Studies for her recommendations for revisions.

The author is grateful to Douglas Newandee, who motivated her to attain new depths of knowledge.

The author thanks Frank Vento, whose love and friendship sustained her during this research and empowered her to 'take this test.'

TABLE OF CONTENTS

TABLE OF CONTENTS
(Continued)

LIST OF TABLES

LIST OF FIGURES

CHAPTER 1

PHYSIOLOGICAL BACKGROUND

This chapter will serve as a brief overview of the biological basis of the electromyographic signals used in this study, as well as an overview of the systems used to acquire this data. Understanding the interaction of the region of the brain that is stimulated with the muscle whose activity is being measured is critical to deciphering the currently undefined role of the central nervous system in the modulation of jaw muscle recruitment. This chapter details both the physiological systems evaluated and the methods by which the data were acquired.

1.1 Statement of Objective

The objective of this research is to assess and more clearly define the differences in muscle recruitment patterns in the masseter (jaw) muscle during two behavioral states: during emotional stress and during simulated mastication (eating). The cat was chosen for this experiment due to a stereotyped emotional response, referred to as "affective defense," which includes retraction of the ears, unsheathing of the claws, vocalization (hissing), significant pupillary dilation and arching of the back. The response was generated by electrically stimulating specific sites of the hypothalamus that are known to elicit this particular behavioral response [1]. The comparison between these two behavioral states will yield further insight into the difference in muscle recruitment patterns of voluntary versus emotionally-elicited muscle recruitment.

Analyses of the EMG obtained during the two behavioral states have been limited in the past to either time or frequency analyses. This research presents an application of the time-frequency decomposition, known as a wavelet multi-resolution analysis, to the EMG obtained during the two behavioral states. This objective of this analysis is the production of a better definition of the role that stress, in this case produced directly from stimulation of the region of the brain that is known for initiating the stress response, plays in modulating the recruitment of jaw muscle activity. It is believed that stress plays an important role in the onset of TMD. It is therefore important to understand how this emotional state alters muscle activity and recruitment. This will enable a clearer understanding of the neuronal mechanisms behind this disorder and ultimately, will aid in the development of better diagnosis methods and treatments for TMD.

This study was accomplished by a comparative analysis of the EMG signals obtained at the masseter muscle during two behavioral states. This thesis will provide a brief overview of traditional methods of analysis, including independent time and frequency methods, and compare the results to a more detailed time-frequency analysis using the wavelet transform. This research will detail the wavelet transform and perform, for the first time, a time-frequency decomposition of EMG signals obtained at the jaw muscle during two behavioral states, during stress versus during voluntary activity. A filtering program was written in Labview to remove DC as well as frequency levels over 750 Hz. The program also removed the frequency band from 57.5 to 65 Hz, to remove both 60 Hz noise, and the 62.5 Hz stimulation signal. A program was developed using the Matlab wavelet toolkit that employs the DauBechies family of wavelets with order of 6 to perform the continuous wavelet transform. The time frequency analysis enables the

researcher to evaluate various frequency bands over all time in the duration of the signal. This enables the detection of transient changes in the frequency content of the signal that were impossible to capture using traditional power spectrum techniques, which averaged the frequency content over all time of the signal. It is this transient detection, coupled with the ability to investigate changes in frequency over time, which makes the wavelet time frequency analysis ideal for this research.

1.2 The Hypothalamus and Pituitary Hormones

"It would be difficult to overstate the influence of hypothalamic and pituitary hormones over physiologic processes" [2]. The main function of the hypothalamus is maintaining homeostasis, the process by which the body regulates all functionality. It monitors and reacts to changes in blood pressure, gut distension, body weight, taste, smell, metabolism, reproductive organ functionality, ionic balance, fluid and electrolyte levels, skin temperature and stretch, circadian rhythms and many more control systems of the body. The hypothalamus is located on either side of the third ventricle, below the thalamus, as shown in Figure 1.1.

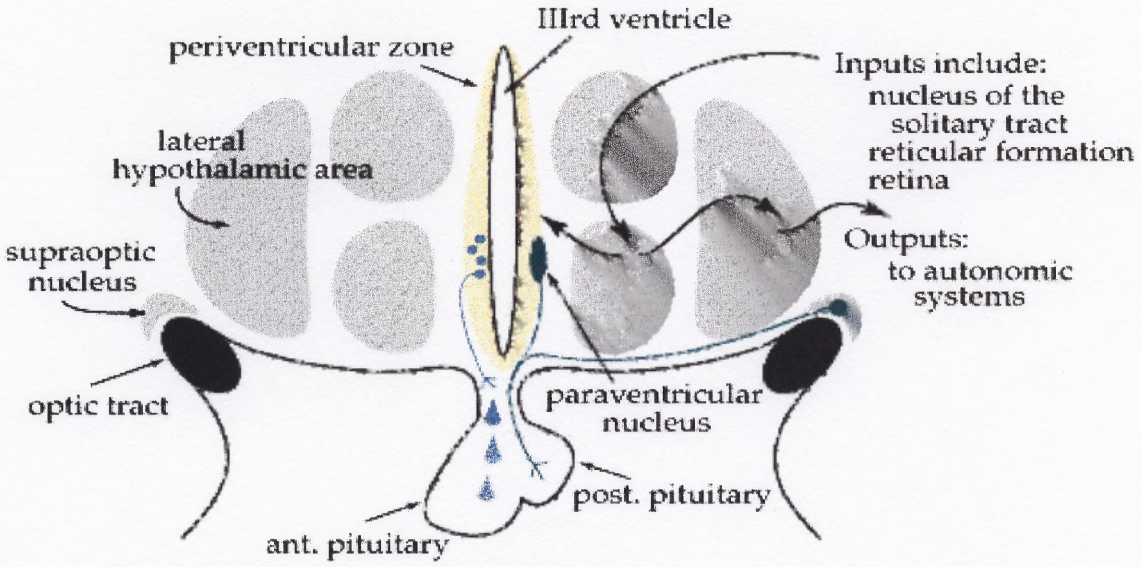

Figure 1.1 Location and interplay between Hypothalamus and Pituitary gland.

The hypothalamus reacts to changes in any of these systems in either or both of the following ways: through electrical signaling to the autonomic nervous system and chemical signals via the pituitary gland, which is also known as the hypophysis [3]. Electrical signals include projections to the Vagus nerve, which is a part of the parasympathetic nervous system, as well as stimulation of regions in the spinal cord associated with synaptic activity. In this way, the hypothalamus controls the function of both components of the autonomic nervous system.

The hypothalamus innervates the posterior pituitary directly, which stimulates the release of hormones such as oxytocin and vasopressin into the bloodstream. The hypothalamus may also control the systems chemically by sending hormones to the anterior pituitary gland, which in turn stimulates the release of hormones such as thyroid-stimulating and leutenizing hormones, among others, into the bloodstream. The

hypothalamic-pituitary interaction can be seen in Figure 1.2. These reactions are observed in situations where the subject is placed under stress. It is in these ways that the Hypothalamus plays a critical role in the stress response of the human body.

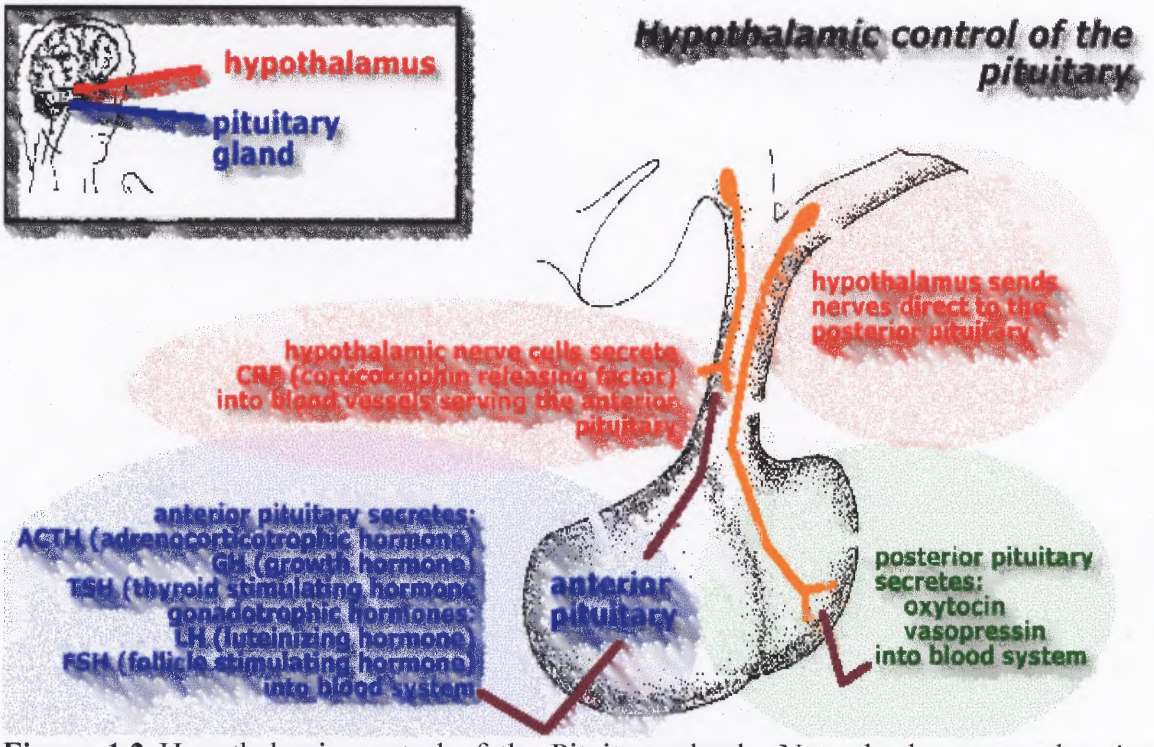

Figure 1.2 Hypothalamic control of the Pituitary gland. Note the hormones that Are released as a result of stimulation from the hypothalamus.

1.2.1 Stress and the Stress Response

It is important to have a clear understanding of the term stress in the context of this project. In this research, the term stress response refers to the physiological reaction of an animal or human to changes in its environment, such as the release of CRH and oxytocin. Stressors are the stimuli that create the stress response. These stressors can be any or a combination of a variety of events, such as a change in temperature or the anticipation of a mental stress, such as an exam [4].

The stress response, initiated in the Hypothalamus, is thought to modulate the muscle activation pathway followed during voluntary muscle activity. The planning and control of ongoing voluntary movements is dictated primarily by the Cerebral Cortex and Cerebellum, and through interactions between the structures beneath the cortex, referred to as subcortical nuclei, and the cortex. This pathway that controls voluntary activity of the masseter muscle is also active during stress. However, the stress response that is initiated during Hypothalamic stimulation interacts with this pathway to modulate the muscle activity. It is unclear how this modulation occurs during the stress response.

1.3 Temporomandibular Joint Disorder

The temporomandibular joint (TMJ) and masseter muscle are the main anatomical focus of this project. The temporomandibular joint connects the mandible, or jaw, to the fixed temporal bone in the cranium. The rounded edges of the mandible that connect to the skull are called condyles. As is common with every joint in the human body, there exists a disc between the condyles and temporal bone. These cushioning discs, referred to as the articular discs, where articular simply means "joint," exist to absorb shock from jaw movements and to ensure that the condyles slide easily along the temporal bone. The masseter muscle is a rectangular skeletal muscle that controls the movement and position of the jaw, in terms of rotation and extension. Figure 1.3 illustrates the anatomy of this region in the human [5]. The TMJ area in the cat is similar to that of the human and although the type of muscle fiber is different between the two species, the masseter muscles function in a similar fashion.

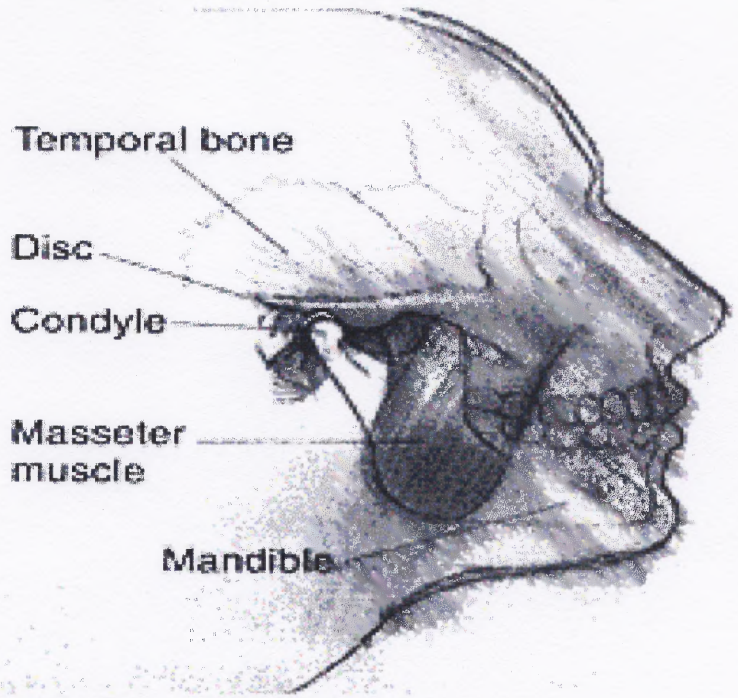

Figure 1.3 Anatomy of the Temporomandibular Joint.

The etiology of temporomandibular dysfunction (TMD) is undefined. In addition, there are many treatments that address the symptoms of the pain, but do not address the underlying source of the malady. It is challenging to find two sources that agree about the cause and treatment of this malady. This is due, in part, to the fact that the mechanisms underlying jaw muscle hyperactivity, which is believed to be a main contributing factor in TMD, are not well defined.

1.3.1 Symptoms of TMD

TMD is associated with a variety of symptoms. Some of these symptoms include limited ability to open the mouth, popping, grating or clicking sounds when the jaw is opened or closed, limited jaw movement, quick fatigue of the jaw muscle during normal activity, headaches, earaches, pain in the neck and shoulder areas and locking of the jaw [6].

Bruxing behavior, or grinding of the teeth, is also a common nighttime activity of patients diagnosed with a TMD. It is unclear whether the bruxing behavior causes the pain in the jaw muscle, or if the hyperactivity of the jaw muscle is what causes the bruxing behavior in these patients [7].

Temporomandibular disorders generally fall into three main categories: myofacial pain, internal derangement of the joint and degenerative joint disease. Myofacial pain is the most common form of TMD. This includes pain in the neck and shoulder muscles, as well as in the muscles that control jaw position and movement. Internal derangement refers to displacement of the articular disc (refer to Figure 1.3). This term describes any abnormal configuration of the articular disc, articular eminence and the mandibular condyle [8, 9]. Inflammatory and degenerative diseases of the TMJ primarily affect the articular surfaces and commonly are forms of degenerative arthritis, degenerative joint disease, osteoarthritis and osteoarthrosis. To confound the diagnosis and treatment of a TMD further, it appears that all three types of TMD have the same symptoms. The symptoms may include some or all of the following: clicking, grating or popping sounds in the temporomandibular joint, ringing or hissing in the ears, tightness in the jaw, neck and shoulder muscles, headaches, dizziness, locking of the jaw in either or both the open or closed positions, grinding of the teeth, limited opening of the mouth and difficulty hearing.

1.3.2 Causes of TMD

Symptoms and causes of TMD vary between patients, with no single root cause defined. Severe injury to the jaw or TMJ may cause a TMD. The form of TMD resulting from a traumatic blow to the joint is most likely a dislocation of the disc. The ligaments keeping

the disc in place can only be stretched a certain amount before they lose the ability to heal themselves and return to normal positions. In the event of a sudden forced large movement of the mandible, the disc can be displaced or damaged, or the bones of the joint may be damaged and cause the resultant dislocation. Less immediately, arthritis or some other form of degenerative TMD can occur from an injury. The cause of myofacial pain is unclear. Some experts feel that this is a result of mental or physical stress causing the skeletal muscle in the TMJ to contract more frequently and powerfully than in people not suffering from a TMD [7].

1.4 Skeletal Muscle and Electromyography

Contraction of skeletal muscles is accomplished through central nervous system interaction with motor nerve fibers, which innervate muscle fibers. A motor unit consists of a motoneuron and the muscle fibers that it innervates. Impulses are generated in the motoneuron and propagate to the fibers of the motor unit. It has been observed that force of contraction is related to the frequency of the action potential and the number of motor units that are recruited [10]. Measurements of the electrical events associated with muscle contractions are known as electromyographic (EMG) recordings. These measurements may give insight into the activation, or recruitment, pattern of the muscle. For instance, fast firing muscles will display higher frequency content in the EMG recordings due to the higher frequency of the impulses that it receives, whereas slow firing muscles would create a lower frequency content in the signal. Patterns of high and low frequency components in the signal may indicate the recruitment pattern of the various types of muscle fibers during a contraction, as well as provide indications of

fatigue [11, 12]. Fatigue has been measured, in purely frequency analyses, as the point at which the median frequency decreases. Dolan, et al. suggest that the increase in power in the low frequency range (5 – 30 Hz) has been found to be a more precise method of detecting muscle fatigue.

A muscle fiber "twitch" is defined as the mechanical response of a single fiber to a single action potential. There is a delay between the time when the electrical impulse stimulates the muscle fiber and the mechanical contraction of the muscle fiber. Once initiated, the mechanical contraction, or "twitch," may last up to 200 ms, while the action potential may last only 1-2 ms. The difference in reaction times enables the motoneuron to initiate a second impulse before the mechanical response to the first impulse has ended. This addition of electrical impulse before the mechanical activity has completed is known as summation. This results in a higher muscle tension during the time period that the electrical stimuli occur before the mechanical response of the fiber has ended, as is illustrated in Figure 1.4.

This summation of fiber activity has a saturation point. This is the point at which increased frequency of the action potential relative to the duration of the muscle twitch will no longer cause an increase in tension. Rather, the muscle reaches a saturation point which varies depending upon whether the fiber is fast or slow firing, as well as upon the diameter of the fiber itself [13].

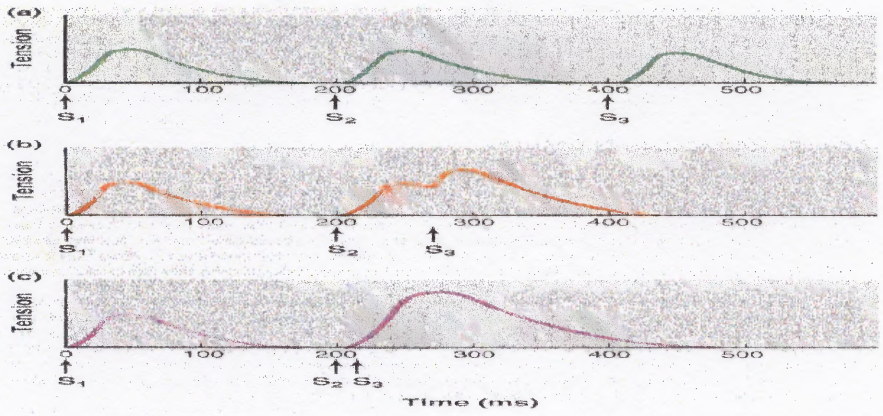

Figure 1.4 Summation of action potentials. Illustration of potentials that occur before the muscle twitch has ended and the resultant summation of muscle tension. S_1 and S_2 are the two stimuli. Note the increase in tension as the time between stimuli decreases.

An electrode placed parallel to the muscle of interest can detect the electrical impulses present during the muscle twitch. These potentials can be positive or negative, and as a result, the electromyographic signals captured during muscle activation contain both positive and negative, or polarized, components at any point in time. The recorded response of a motor unit has an amplitude of 0.1 – 5 mV. The frequencies present in EMG signals typically have a range from DC to 10 kHz, depending upon the diameter and type of muscle fiber that is being measured [14]. In this study, the data files were band passed from 2 to 750 Hz to remove DC voltage and to avoid any biasing effects. A biasing effect occurs when the sampling frequency is too low for the largest frequency content in the signal. The Nyquist sampling theorem states that in order to avoid biasing effects, the introduction of rogue frequency components into the signal, the sampling frequency must be at least twice as large as the highest frequency component (F_{max}) contained in the signal. In this case, the largest frequency component allowed to pass through the filter is 750 Hz. The signal was sampled at 2000 Hz, well over the $2*F_{max}$ (in this case after filtering, equivalent to 1500 Hz) limit imposed by the Nyquist sampling

theorem. The data files were further notch filtered from 57.5 to 65 Hz to remove any 60 Hz or stimulation artifact that may have been introduced into the recordings. The program that performed the filtering is written in Labview version 5.1. Both the front and wiring panels of the filtering program are included in Appendix A.

CHAPTER 2

EXPERIMENTAL PROCEDURES AND METHODS

The data used in this experiment were previously obtained by Weiner, et al., at the Limbic Research Laboratory at the Department of Neurosciences, New Jersey Medical School in Newark, New Jersey. The results of the previous data analysis were reported in the Journal of Dental Research. This chapter provides the details of the experiment, including subject background, equipment configuration, stimulation techniques and data analysis methods.

2.1 Subject Background and Preparation

Two healthy adult cats of both sexes, weighing 2.5 to 4.0 kg, that did not spontaneously attack rats, were used in this experiment. The animals were deeply anesthetized using sodium pentobarbital, and six guide tubes were placed bilaterally over the medial and lateral hypothalamus according to the stereotaxic locations of Ajmone-Marsan [15]. The guide tubes were then cemented into place using dental cement. Moveable monopolar electrodes coated to within 0.5 mm of the tips were lowered in 0.5 mm increments through these guide tubes into the hypothalamus, with electrical stimulation being applied to identify the sites that elicit the desired behavioral response. When a reliable, or repeatable across ten trials on more than 50% of the animals, behavioral response was elicited, the electrodes were cemented into place using dental cement.

2.1.1 Behavioral Response Attainment

As the electrodes were being incrementally lowered into the hypothalamus, stimulation signals ranging from 0.2 to 0.6 mA were applied to determine sites where the affective defense response could be obtained. Prior to the experiment, the cat was allowed an acclimation period in which it was allowed to move freely in the 70 x 70 x 60 cm wooden observation cage with a clear plastic front. During the experiment, the cat was awake and allowed to move freely in the observation cage. The applied stimulation consisted of biphasic rectangular pulses ranging from 0.2 to 0.6 mA at 62.5 Hz and 1ms per half cycle duration. The stimulation pulses were generated by two independent S-88 Grass Instrument stimulators. The stimulation signal was carried to the subject using stimulus isolation units. The peak-to-peak current was monitored with an oscilloscope (502A, Tektronix, Beaverton, OR). When a desired response was elicited from a site, baseline threshold values were determined employing the Methods of Limits, wherein a series of ten descending and ascending current levels were employed. The current levels were adjusted in increments of 0.05 mA in a counterbalanced A-B-B-A configuration to avoid order effects which would confound the data analysis. The threshold behavioral response occurs at a value at which more than 50% of the animals displayed a behavior that is consistent across ten trials. A current 0.05 mA above threshold was utilized for this research. Stimulation levels above this were observed to cause undue fatigue to the animal during the experiment. When a reliable response was elicited, the electrode was cemented into place inside the guide tubes with dental cement.

2.2 Experimental Protocol

During the experiment, the animal was awake and gently restrained in a loose fitting bag to reduce the chance of the animal removing the electrodes that were attached to its jaw and skull and to reduce the risk of harm that the animal might do to itself. The EMG signal was recorded during two different behavioral conditions: during stimulation of the hypothalamic sites from which the desired behavioral response was elicited and during simulated mastication. Having the animal bite unilaterally on a stick simulated mastication.

Each session was 45 minutes in length. Trials of electrical stimulation were separated by two-minute rest periods. The stimulation trials lasted no longer than 20 seconds each, and only one stimulation site was tested per session. The experiment consisted of a series of ten alternating trials of stimulation and stick biting, which were performed using the A-B-B-A paradigm to avoid order effects.

2.3 Data Acquisition

EMG recordings were obtained using surface silver-silver chloride disposable electrodes. (Myotronics Research, Seattle, WA). The skin overlying the master muscle was shaved and dried with alcohol and the electrodes were placed 15 mm apart on the surface of the skin and were affixed to the skin using collodion. The electrodes were placed directly above and parallel to the orientation of the masseter muscle fibers. Recordings were taken bilaterally from the masseter muscle. A ground electrode was placed on the skull. The EMG signals were preamplified and recorded using a Grass CP511 amplifier (Grass-Telefactor, West Warwick, RI) that rectified and integrated the signal. The data were

then converted to digital signals and imported to a Gateway 400 MHz PC via the National Instruments data acquisition card, NI PCI-6025E.

2.4 Data Analysis

The evolution of computing technologies has made available the ability to look at data in novel ways and to glean new information about systems that have been studied in the past. The data for this research project have already been assessed in the time and frequency arenas, and a brief overview of the findings from those studies will be provided. These data will now be re-analyzed using the wavelet time-frequency decomposition method. An overview of time-frequency methods is provided in this section. The time-frequency methods of signal decomposition and analysis for this research will be further discussed in Chapter 3.

2.4.1 Review of Time Analysis of Data

Mean EMG voltages were assessed in on this data in a previous study [6]. Findings in this study indicate that the mean value of the EMG signal recorded during electrical stimulation of the hypothalamus was significantly higher than the mean EMG value of the signal recorded during simulated mastication. An analysis of variance also displayed significant differences between the groups, as well [1]. Figure 2.1a illustrates the time representation of the EMG recorded during electrical stimulation, while Figure 2.1b is the time representation of the EMG signal recorded during simulated mastication. Note that in Figure 2.1 a, the stimulation begins with the first large jump in EMG amplitude and ends with the return to the pre-stimulation baseline level. In figure b, mastication is occurring in the locations where the amplitude of the signal is large. Note that the

mastication signal displays gaps in activity, whereas the stimulation file shows no variation in amplitude throughout the course of the stimulation. The magnitudes of the two signals are an order of ten different from each other, intimating significant differences in EMG amplitude between the two behavioral states. Past analyses have included slope analysis and raw EMG magnitude comparisons.

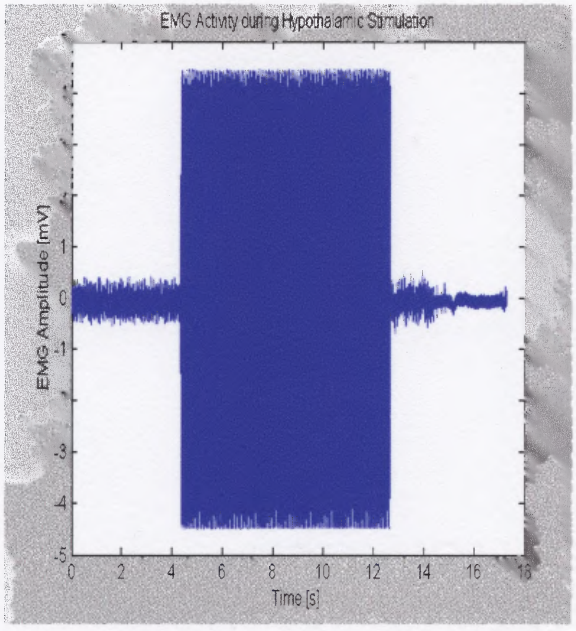

Figure 2.1a Time plot of EMG activity during hypothalamic stimulation.

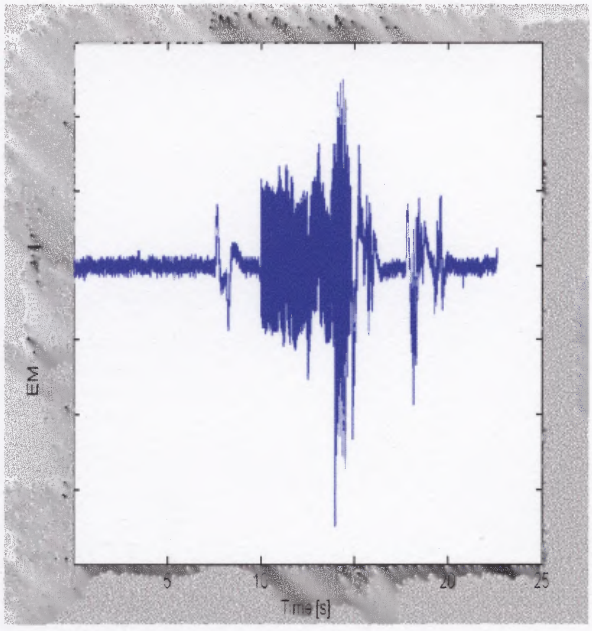

Figure 2.1b Time plot of EMG activity during mastication.

2.4.2 Review of Frequency Analysis of Data

Frequency analysis of this data set has included analyses of mean power frequency (MPF) [16]. This study indicates that there is a marked upward shift in the MPF of the signal during stimulation versus that of the signal during mastication. This suggests that there is an increase in motoneuron firing rate and perhaps a more extensive recruitment of the motoneurons that innervate fast firing muscle fibers in this region. However, the limitation of this method of analysis lies in the loss of time resolution to gain frequency

information, as can be seen in Figures 2.2a and b. In Figure 2.2a, it is clear that during mastication the majority of the frequency power is occurring at less than 50 Hz, with some limited frequency activity in the higher frequency ranges. In Figure 2.2b, it is clear that there are bands of high power frequency activity occurring throughout the signal, with the largest activity occurring in the 150-300 Hz range. It is unclear from these images when various frequencies are the most active It is also unclear whether all frequencies are present at all times, with different power levels, or if there are high power frequency components present at isolated times within the signal. Both of these problems arise because the mean power gives time-averaged frequency information. This removes the time resolution of the signal, rendering it impossible to assess when various frequency components are the most active throughout the signal.

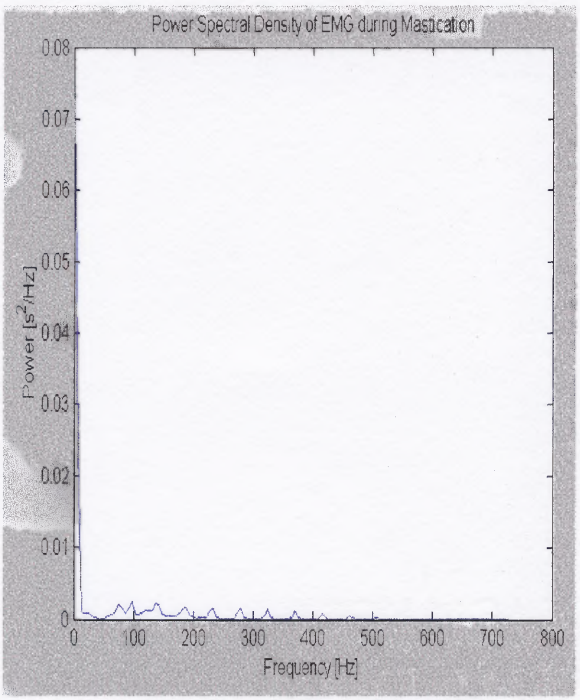

Figure 2.2a Power Spectral Density of EMG activity during Mastication.

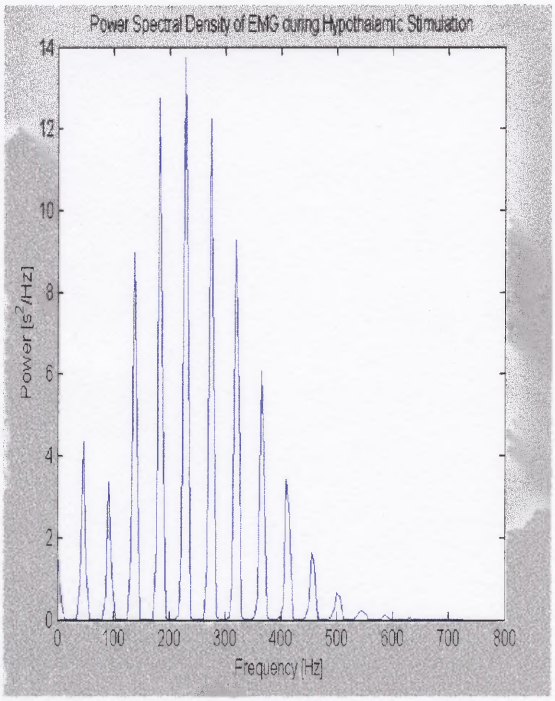

Figure 2.2b Power Spectral Density of EMG activity during hypothalamic stimulation.

Previous studies have uncovered a significantly elevated power of the frequency activity in the stimulation files as opposed to the mastication files [1, 16, 17]. Until now, it has been unclear whether the upward shift is a result of more fast-firing muscle fiber activation or simply an increase in firing rate of the motor neuron. A higher power at a specific frequency would indicate that the change is indicative of the first situation, where there is an increase in the number of motoneurons being recruited and resulting in a shift in MPF. If, however, there is a shift in frequency that does not contain a shift in power of the frequency content, then the implication is that the firing rate of the motor neurons is increasing. Unfortunately, this information was unavailable for analysis in the past, due to limitations in computing and analysis power.

2.5 Time-Frequency Analysis using the Continuous Wavelet Transform (CWT)

The EMG signals in this study were sampled at a rate of 2000 Hz. They were run through a Labivew program that removed the DC component and the chance for a biasing effect by bandpassing the data from 3 to 750 Hz, as per the Nyquist sampling theorem. As can be seen in Figure 2.2, the majority of the power in the signals elicited from both behavioral states is centered at less than 200 Hz. The data were also filtered from 57.5 to 63 Hz to remove stimulation and 60 Hz noise artifacts. The filtered EMG files were then run through the Matlab wavelet program outlined in Appendix B to perform the continuous wavelet transform on the signal. This analysis employs the Daubechies order 6 (DB6) wavelet. The rationale for choosing this particular wavelet, as well as a discussion of wavelet technique, is the topic of Chapter 3.

CHAPTER 3

WAVELET TIME FREQUENCY ANALYSIS

Studies that have examined the role of the nervous system in the modulation of the recruitment of muscles have been limited to the evaluation of electromyographic signals in either the time or frequency domains [1, 16, 17]. These studies have yielded valuable information about the role of hypothalamically induced neuromuscular activity in comparison to cortically invoked activity. Results from these studies indicate that the values of EMG amplitude and mean power frequency obtained during hypothalamic stimulation were significantly higher than those observed during mastication. The studies have thus indicated that there is a correlation between hypothalamic stimulation and increased EMG activity in both time and frequency measures. It is thought that the shift in mean power frequency is indicative of a more extensive recruitment of rapidly fatiguing muscle fibers, as well as an increase in motor neuron firing frequency. However, previous studies have not been able to clearly define the role of the nervous system in the modulation of the recruitment of the fibers of the masseter muscle. This is because at the time the studies were performed, the computing capability and signal analysis techniques were limited. This resulted in the lack of either time or frequency resolution, depending upon the type of analysis performed.

The hypothalamus is thought to activate the stress response and thereby modulate the level of activity in the masseter muscle, which is controlled mainly by the cortex and basal ganglia during voluntary muscular activity. The past studies have been limited in the respect that the data analyses in the time domain are missing critical information

regarding the frequency content of the signal, whereas the frequency analyses are missing time resolution. The studies were able to identify that in the time domain the amplitude of the EMG signal changed at specific times during the experiment. They also identified that the average power of the frequency was different between the two behavioral states. This indicates that the muscle activity varies between the two behavioral states, but is not enough information to clearly define what is causing the changes in EMG amplitude at specific times. It is also not enough information to clearly define what is causing the changes in mean power frequency. The averaged power only accounts for specific frequency content that is averaged over the length of the signal, as shown in Figures 2.2 a and b. This gives an indication of which frequencies are the most active in the signal, but it does not give time information that would indicate what frequencies are active at which times. A combination of time and frequency information would elucidate the ways in which the muscle recruitment is modified by the stress response.

A method of combining the two attributes of time and frequency without losing critical time or Fourier parameter information is through the implementation of a time-frequency decomposition. This method of evaluating non-stationary signals that contain transient components has been gaining increasing popularity, with the first implications for applications to signal analysis in the 1940s. Recently, a time-frequency method has come to the forefront as a powerful method of analyzing transients and allowing the researcher to investigate frequency components over the length of the signal. This method, known as the Wavelet Time-Frequency Multi-Resolution analysis, makes it possible to have good time and frequency resolution due to a shape that is other than a sinusoid and is applied to the signal using a scalable window.

A shortcoming of time-frequency decompositions based upon the Fourier transform is the inability to use a scalable window, which results in the loss of time resolution. The Fourier transform based methods of time frequency analysis are based upon scaling and shifting a sinusoid and convolving it with signal to be analyzed, using a fixed window of time for all frequencies. Another shortcoming of this method is that because sinusoids are infinite signals in time, they are not contained completely in the window that is chosen for the analysis. For this reason, the use of a sinusoid introduces artifact into the analysis due to the fact that the window captures different quantities of periods of the sinusoid at different frequencies, depending on window size being used.

The wavelet transform uses the theory of time-frequency decomposition and employs an adaptive window size that changes based upon the frequency being examined. It also employs basis signals other than sinusoids in the analysis. The basis signals for this type of analysis are called wavelets. The signals employed in the wavelet analysis decay to zero exponentially, reducing the problem of the base extending outside of the window and the associated introduction of artifact. They also oscillate about zero in the time domain and therefore possess a zero mean value. Translated to the frequency domain, the Fourier transform of the wavelet must approach zero at the zero frequency, which forces a band-pass behavior of the wavelet. This time and frequency characteristic of the wavelet is referred to as the *admissibility condition*, which must be met in order for reconstruction of the signal using wavelet coefficients [18]. The requirements for wavelet construction and implementation are discussed in detail in Section 3.2.2.

The Fourier transform utilizes the infinitely bound sine wave as the basis for analysis. This enhances the likelihood of missing small transients in signals that the

wavelet would detect due to its limited duration. The wavelet, then, is well suited to analyze a local area of a signal that would otherwise be missed by the traditional Fourier analysis. The shape of the wavelet is typically asymmetrical as compared to the Fourier transform, which utilizes the uniformly shaped sinusoid. The shape of the wavelet renders it well suited to detection in signals that contain sharp changes in frequency content.

Another quality of the Daubechies family of wavelets that makes them useful techniques in non-stationary signal analysis is that they are orthogonal. This attribute causes the wavelet coefficients to be orthogonal. In turn, this causes each wavelet coefficient to be representative of independent signal components [19]. For example certain wavelets, such as the Morlet, Gaussian and Mexican Hat, are not orthogonal.

The wavelet method is unlike other time-frequency decomposition methods because it is not based upon the traditional Fourier base of sinusoids and does not use fixed windows of time to analyze the signal at all frequencies. The window size varies depending upon the scale, or frequency, that is being investigated. In addition, the wavelet method convolves a "mother wavelet," of shape and duration varied by the class of wavelet and the scale being assessed, with the signal to be analyzed. This mother wavelet is scaled and shifted based upon the frequency band of interest. This scaling and shifting allows for the detection of small transients as well as larger trends within the data. It also allows for better time and frequency resolution that traditional methods have provided. A wavelet analysis is the method chosen for this work. The construction and implementation of the Continuous Wavelet Transform will be discussed in this chapter.

3.1 History of the Wavelet Transform

The wavelet time frequency decomposition is a mathematical theory that has been in development since the early 1900s. Alfred Haar, in 1909, is credited with the first written description of the theory that has since become referred to as wavelet analysis. Since then, the theory has gained increasing popularity. In 1988, Stephane Mallat derived the algorithm that is the basis for this approach to time-frequency analysis [20]. Since then, engineers have embraced this method in various fields of research, including but not limited to acoustic emission [21,22], transmission line fault detection and protection [23] and detection and classification of material attributes [24]. Recently, biomedical applications of the wavelet analysis, such as the analysis of motor unit action potentials [25] and the use of electromyography for the detection of back muscle fatigue [11], began to appear in the literature.

The theory of wavelet based decomposition of signals is founded upon the nineteenth century theory presented by Joseph Fourier, which has come to be known as the Fourier analysis or Fourier transform, whereby a signal is decomposed into its frequency components via the use of sinusoids. The wavelet transform replaces the time information lost in the Fourier transform. Wavelet analysis performs a frequency analysis that assesses frequency band activity over time, rather than calculating the sum of all frequency activity during the life of the signal of interest. Today, United States mathematicians, such as Daubechies and Coiflet, lead the research that is aimed toward the advancement of wavelet theory [20].

3.2 Implementation of the Wavelet Transform

The Continuous Wavelet Transform (CWT) uses a main signal, referred to as the "mother wavelet" and convolves a shifted and scaled version of this signal with the signal to be analyzed. Mathematically, this approach is represented by the equation

$$C(a,p) = \int_{-\infty}^{\infty} f(t)\psi^*(a,p,t)dt \tag{3.1}$$

where ***C*** represents the coefficients that are a result of the product of the original function and the conjugate of the mother wavelet, ***a*** represents the scaling factor of the mother wavelet, ***p*** is the shifting factor of the mother wavelet, ***f(t)*** is the original signal and $\psi^*(a,p,t)$ is the conjugate time-dependant mother wavelet, scaled and shifted by ***a*** and ***p***, respectively. The mother wavelet is decomposed via scaling and translation into a set of smaller basis functions, represented by ψ_{ap}, where

$$\psi_{ap}(t) = \frac{1}{\sqrt{a}}\psi\left(\frac{t-p}{a}\right), \tag{3.2}$$

and $a^{-1/2}$ provides energy normalization across scales.

Scaling is the process by which the wavelet is stretched or compressed at a certain level, as seen in Figure 3.1. This scaling or compressing enables the wavelet to capture frequency information at various frequency levels. Higher frequency content is captured at lower scales and conversely, lower frequency content is captured with higher scales.

Scales are in powers of 2. For example, a scale factor of 9 corresponds to a level of 2^9, or 512, wavelet coefficients. At higher scale levels the wavelet analysis possesses greater

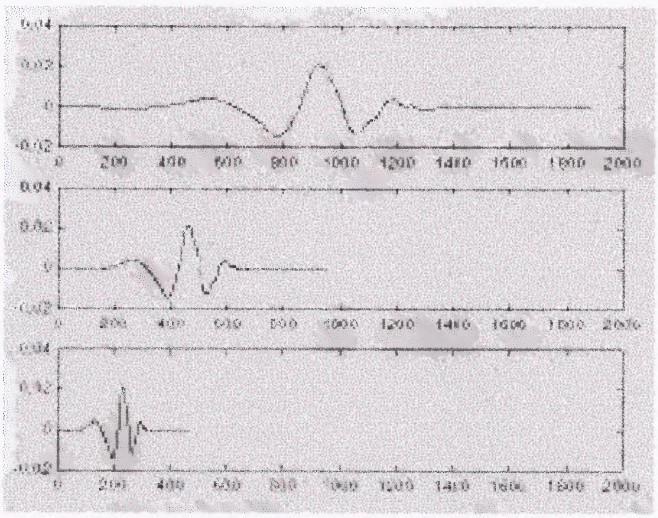

Figure 3.1 Scaling the mother wavelet. Note that the signal becomes increasingly short in duration at smaller scales. This yields information about quickly changing, or the high frequency content of, signals.

frequency resolution, whereas lower scale levels yield better time resolution because decreasing the scale parameter increases the width of the wavelets, as shown in Figure 3.2 [26]. The bandwidth decreases by half at every scale. This enables higher frequency resolution at higher scales, or lower frequencies. Conversely, it enables higher time resolution at lower scales, or higher frequencies. Wavelet representations are typically referred to as time-scale decompositions due to the fact that the mother wavelet is compared to the original signal in scales, not frequency.

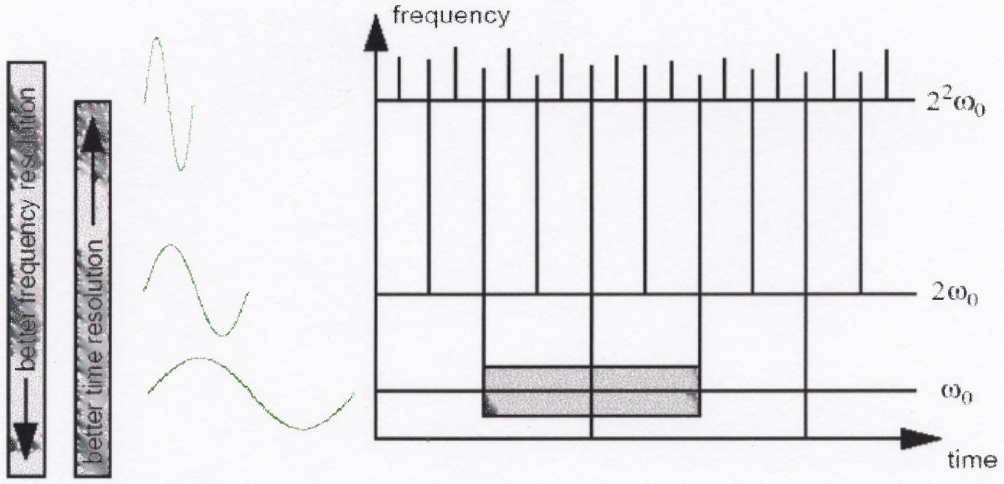

Figure 3.2 Wavelet transform scaling grid. Scale is approximately equivalent to the inverse of frequency. Note that scale increases in the opposite direction of the frequency. As frequency increases, scale decreases. As the scale decreases, the duration of the wavelet decreases, enhancing the time resolution of the wavelet at higher frequencies.

However, frequency roughly correlates to the inverse of the scale value and is related to the scale in the following way:

$$F_a = \frac{F_c}{F_s a}, \tag{3.3}$$

where F_a is the frequency correlating to a specific scale, F_s is the sampling frequency, F_c is the center frequency of the specific mother wavelet at the scale being analyzed and a is the scale being analyzed. The scaled wavelet is then shifted across all time of the signal.

Shifting is the process by which the onset of the application of the mother wavelet is delayed or hastened, as can be seen in Figure 3.3 [20]. This allows for the time component in the wavelet analysis. Rather than looking at specific windows of time, the wavelet analysis looks at all time in the duration of the signal being analyzed, at varying

scales. Higher scales will yield larger shifts in time in order to capture the activity at lower frequencies. Likewise, lower scales will yield smaller shifts in time, which will capture the higher frequency, or rapidly changing, content of the signal.

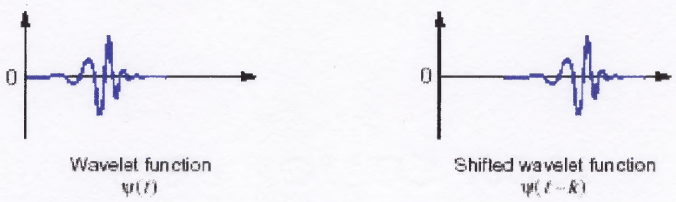

Figure 3.3 Shifting the mother wavelet. In this case, ***k*** is the shifting factor, or the length of time by which to delay the onset of the application of the wavelet.

Wavelets address problems with inaccuracies of representation of the frequency content of a signal as a result of Fourier analysis based time-frequency analyses. It does this by convolving the signal to be analyzed with a signal that meets two specific properties: the *admissibility* and the *regularity* conditions. The admissibility condition requires that the wavelet decays quickly to zero outside of the time and frequency of interest. This property of wavelets is known as the *localization property* of the wavelet. In the time domain, this is equivalent to saying that the wavelet must oscillate about zero and have a mean value of zero. In the frequency domain, this is equivalent to the statement that the wavelet is *compactly supported,* or *band limited*, and must decay quickly to zero outside of the frequency band of interest. This concept is represented mathematically in Equations 3.4 and 3.5.

$$\int \psi(t)dt = 0 \tag{3.4}$$

$$|\psi(\omega)|^2_{\omega=0} = 0 \tag{3.5}$$

That is, the mother wavelet signal exists only in the local region of the signal. These two combined attributes of the wavelet transform are collectively referred to as the *admissibility condition*, which is part of the requirement that must be met for the signal to be considered a wavelet.

The fact that wavelets decay in both the time and frequency domains results in an analysis that possesses very good time and frequency localization. However, it is impossible to have perfect accuracy of analysis due to Heisenberg's uncertainty principle. In the application of this theory to signal analysis, the principle states that it is impossible to obtain information about an exact frequency and exact time at which that frequency occurs. That is, it is impossible to get exact information about both time and frequency for any given time or frequency [27].

The regularity condition, which is the other portion of the requirement for a signal to be considered a wavelet, states that wavelet transforms must decay quickly with decreasing scale and employs the concept of vanishing moments. The concept of vanishing moments can best be described as the points at which the derivatives of the function are equal to zero. Equation 3.6 defines the moment, M_p, of the wavelet as

$$M_p = \int f^p \psi(t) dt \,, \tag{3.6}$$

where f^p is the pth derivative of f and $\psi(t)$ is the wavelet. Recall from Equation 3.4 that M_p equals zero, based upon the above equation. Expanding Equation 3.1 to the nth term using a Taylor expansion yields

$$C(a,0)=\frac{1}{\sqrt{a}}\left[f(0)M_0a+\frac{f^{(1)}(0)}{1!}M_1a^2+\frac{f^{(2)}(0)}{2!}M_2a^3+\ldots+\frac{f^{(n)}(0)}{n!}M_na^{n+1}+X(a^{n+2})\right], \tag{3.7}$$

where the translation, or shifting, coefficient p is set to zero for simplicity and X is the remainder of the expansion [30]. Implementing Equations 3.4 and 3.6, the terms with moments approach zero and the value of the wavelet transform coefficients decay as fast as a^{n+2}. The higher n is, the faster the signal decays. This is what is meant in wavelet analysis by the *regularity condition.* That is, as the number of vanishing moments increases, the shape of the wavelet becomes smoother, or more *regular.* The number of vanishing moments is equivalent to n. For the Daubechies family of wavelets, n is theoretically infinite, rendering the wavelet ideal for many diverse applications.

In summary, the wavelet should meet the conditions of admissibility and regularity. The admissibility condition allows the wavelet to be used in applications where perfect reconstruction of the original signal is necessary. It also ensures that the regularity condition may be met by forcing the moments to zero.

3.3 Use of the Daubechies Order 6 (db6) Wavelet

The wavelet analysis was performed using Matlab version 6.1, with the Wavelet toolbox. The program is included in Appendix B. The data files were filtered as discussed in 2.4.4

using a Labview version 5.1 program, which is included in Appendix A. The EMG data are fast varying signals with transients of short duration.

Lower order Daubechies wavelets are well suited to provide high time resolution in the higher frequency scales [28]. This enables the lower order Daubechies wavelets to capture short transients, which is important when assessing bursts of neuromuscular activity. The transition from levels of higher EMG activity to lower activity may yield important information about motor neuron activation timing, targeting and power. Transient frequency components may also yield insight into the recruitment patterns of the masseter muscle during different behavioral states.

The Daubechies family of wavelets can also be used in continuous or discrete transformations. This is an important aspect to consider, depending upon the desired application. A part of this study assessed whether wavelets could provide an accurate reconstruction of the original signal once decomposed. The Discrete Wavelet Transform (DWT) is necessary for the reconstruction of the wavelet. This is true because the discrete wavelet transform down-samples the signal by a factor of two per scale during the signal decomposition. Down Sampling is necessary because in the wavelet analysis, both the details (high frequency component of the signal at a given scale) and approximations (low frequency content of the signal at a given scale) create a signal that is the same length as the original signal. The difference in numbers of coefficients between the discrete and continuous analyses is illustrated in Figures 3.4a and b. The images illustrate the filtering of the original signal, $\boldsymbol{S}$. The signal is low passed to create the Approximations set of coefficients. $\boldsymbol{S}$ is also high passed to create the details set of coefficients.

In Figure 3.4a, the continuous wavelet transform (CWT), the details and approximations values are not down-sampled. This results in approximation and detail signals that are each the length of the original signal. If the two sets of coefficients from the CWT are combined, the resultant signal contains twice the amount of data as is contained in the original signal.

In contrast, in the discrete wavelet transform (DWT), illustrated in Figure 3.4b, the details and approximations are downsampled by two. The discrete wavelet decomposition removes every other point from the details and approximations, yielding decomposition values that are each half the length of the original signal. Yet, the signal integrity is not lost. Reconstruction of the signal using the discrete coefficient set yields a signal that is equal in length to the original signal.

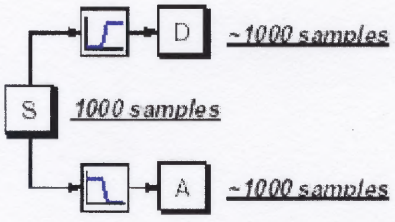

Figure 3.4a Filtering techniques involved with the continuous wavelet transform (CWT).

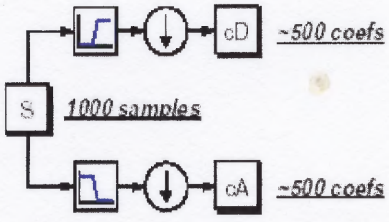

Figure 3.4b Filtering techniques involved with the discrete wavelet transform (DWT).

During reconstruction of the signal, the algorithm needs to upsample the details and approximations signals by a factor of two, as illustrated in Figure 3.5, which can only be done if the original decomposition was done discretely. Upsampling involves placing a zero between discrete points in the details and approximations signals, as shown in Figure 3.6. The resulting reconstructed signal is equal in length to the original signal.

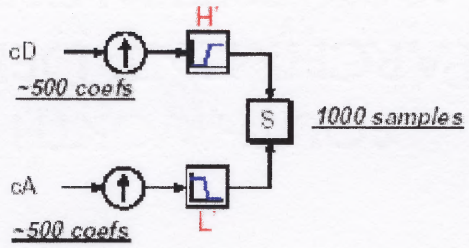

Figure 3.5 Reconstructing the original signal using the DWT coefficients.

The CWT does not provide a signal that can have a zero inserted at every other point and not lose the signal integrity. The CWT yields a smoother frequency analysis and ultimately yields a more complete picture of the frequency activity in the original signal and was thus chosen for the analysis aspect of this research.

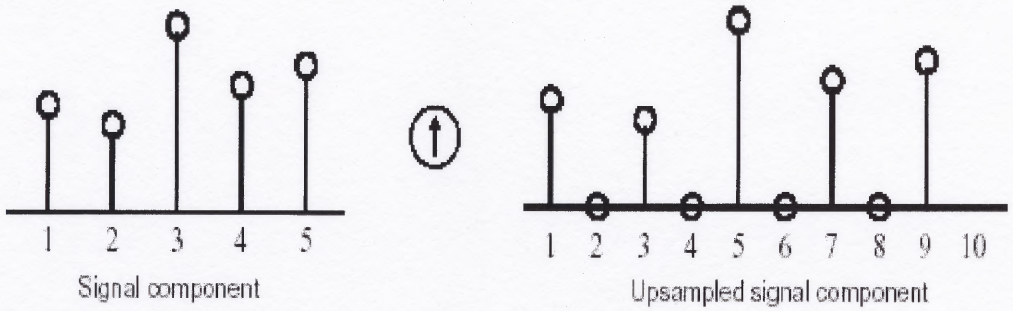

Figure 3.6 Zero insertion between coefficients. The arrow pointing upwards indicates that the upsampling has taken place. Note that the same arrow is present in Figure 3.5, which displays the filtering that takes place during reconstruction.

Figure 3.7 Daubechies Order 6 (db6) wavelet.

A lower middle level Daubechies wavelet, the db6 wavelet, was chosen for this research to ensure the accurate capture of transients and to provide high time resolution of those signal components. The wavelet is defined in terms of six coefficients, and the graph of it is shown in Figure 3.7. In summary, the features of the Daubechies wavelet that made it applicable to this study include compact support, infinite number of vanishing moments, ability to perform both discrete and continuous transformations and high time-resolution at various frequencies.

CHAPTER 4

RESULTS AND DISCUSSION OF ANALYSIS

The analysis of these data was focused in three main categories. First, a comparison of the reconstruction capability of various wavelet types was performed, employing the discrete wavelet transform. Next, a continuous wavelet transform was employed to assess transient components in the signal and perform a visual inspection of the frequency content of the signal during both behavioral states. Finally, in an effort to quantify observations made as a result of the continuous wavelet transform, a comparison of the mean values and area of each scale is performed. This chapter will detail the results of the analyses performed in this research and provide a discussion of these findings in comparison to conclusions reached in previous studies.

4.1 Results of the Discrete Wavelet Decomposition and Reconstruction

As discussed in Chapter 3, a discrete wavelet transformation was performed on the signals, both mastication and stimulation, to determine how well the original signal could be reconstructed from the wavelet coefficients. Theoretically, the wavelet coefficients may be effectively employed to perfectly reconstruct, or yield a 1:1 correlation with, the original signal [19]. This theory was validated by first performing a discrete wavelet decomposition, using various wavelet families, on the signals. The upsampling aspect of wavelet signal reconstruction was then employed to reconstruct the signal. The reconstructed and the original signals were then compared using population correlation calculations, using Equations 4.1 through 4.3, to verify that in fact the two signals are

identical. The correlation calculation is the ratio of the covariance of two data sets divided by the product of their standard deviations. In Equation 4.1, $\rho_{X,Y}$ is the correlation coefficient, which ranges in value from –1 to 1. A correlation of –1 indicates that the two data sets have a slope that is opposite each other, or, as one set increases in value, the other decreases. A value of 1 indicates that the two sets perform in exactly the same way, increasing and decreasing in the same manner. In this research, the values of

$$\rho_{X,Y} = \mathrm{cov}(X,Y)/(\sigma_X * \sigma_Y) \tag{4.1}$$

$$\sigma_X^2 = 1/n * \Sigma(X_i - \mu_X)^2 \tag{4.2}$$

$$\sigma_Y^2 = 1/n * \Sigma(Y_i - \mu_Y)^2 \tag{4.3}$$

the data sets are the same, however a correlation coefficient with a value of 1 does not typically imply that. When looking for frequency changes over time, the amplitude of the time signal is not as significant as the changes in the signal with time. If the two signals present a correlation coefficient of 1, then the two signals have identical frequency characteristics, which is what the research was seeking to identify during the reconstruction testing. In Equations 4.2 and 4.3, μ indicates the mean value, and X_i and Y_i indicate individual data points in data sets X and Y, respectively. The results of the correlation calculation study are displayed in Table 4.1. All wavelets used for this aspect of the research produced a reconstructed signal that had a 1:1 correlation with the original signal except the Discrete Meyer (Dmey) transform, which produced a reconstruction which yielded a correlation coefficient of 0.999994696. Although this value is slightly less than one, the original and reconstructed signals still display a high level of correlation using the Dmey wavelet transform.

Table 4.1 Correlation Results for Discrete Wavelet Transforms

	Original Signal	***Sym2***	***Coif4***	***DB4***	***DB6***	***Dmey***
Original Signal	1					
Sym2	1	1				
Coif4	1	1	1			
DB4	1	1	1	1		
DB6	1	1	1	1	1	
Dmey	0.999994696	0.999995	0.999995	0.999995	0.999995	1

As the name suggests, the discrete Meyer transform is a discretized version of the Meyer wavelet transform. Since the Meyer mother wavelet may not be used for discrete wavelet transformation, a sampled version of it, the Dmey wavelet, is employed for the discrete wavelet transform. The reconstruction using coefficients obtained using the Dmey mother wavelet do not yield a reconstruction correlation value of 1.0 because this wavelet is not the true Meyer mother wavelet, but the discretized version of it. This version of the wavelet was created for the purpose of using the Meyer wavelet in discrete wavelet transforms. The remaining wavelets tested are able to perform both discrete and continuous analyses. Therefore, the Symlet family, order 2 (Sym2), the Coiflet Family, order 4 (Coif4) and the DauBechies family, orders 4 and 6 (DB4, DB6), display a 1:1 correlation between the reconstructed and original signals.

The wavelet used in this research is the DB6 wavelet. As can be seen in Table 4.1, the wavelet has perfect reconstruction capability, which yields a correlation of 1:1 between the reconstructed and original signals, employing this mother wavelet. The DauBechies family of wavelets is capable of performing both discrete and continuous analyses. It has an infinite number of vanishing moments, giving this wavelet good regularity. It decays rapidly outside of the time and frequency of interest, so it meets the

admissibility condition. It has a similar shape to the EMG signal, which is important because the wavelet coefficients are essentially correlation coefficients between the mother wavelet and the signal to be analyzed. The closer the mother wavelet is in shape to the signal to be analyzed, the more highly correlated the results are. This yields higher accuracy in analysis than would be found if the signal was not similar in shape to the mother wavelet. Other characteristics that make this an ideal wavelet to use are the high time resolution at higher frequencies, which make it ideal for capturing transient frequency components in the data.

4.2 Results of the Continuous Wavelet Decomposition

4.2.1 Observations of the CWT coefficients

From visual inspection of the wavelet coefficients, several differences are observed between the EMG activity of the masseter muscle during mastication as opposed to emotionally-mediated activity. Figures 4.1a and b, below, are the three-dimensional plots of the power of the wavelet coefficients versus time and frequency. In both plots, a ridge between approximately 3 and 20 Hz is seen intermittently throughout the duration of both signals. Dolan, et al have suggested that an increase in the power of the frequency activity in the 5- 30 Hz range is an indication of fatigue in the muscle. As can be seen in Figure 4.2, this activity is present almost from the commencement of mastication, the simulated voluntary muscle activity, but the power increases toward the end of the period of mastication. This coincides with the observation that the power shifts from the 300 – 500 Hz frequency band to the 75 – 200 Hz range, indicative of the onset of fatigue in the

masseter muscle. The values are significantly smaller in the mastication files than in the

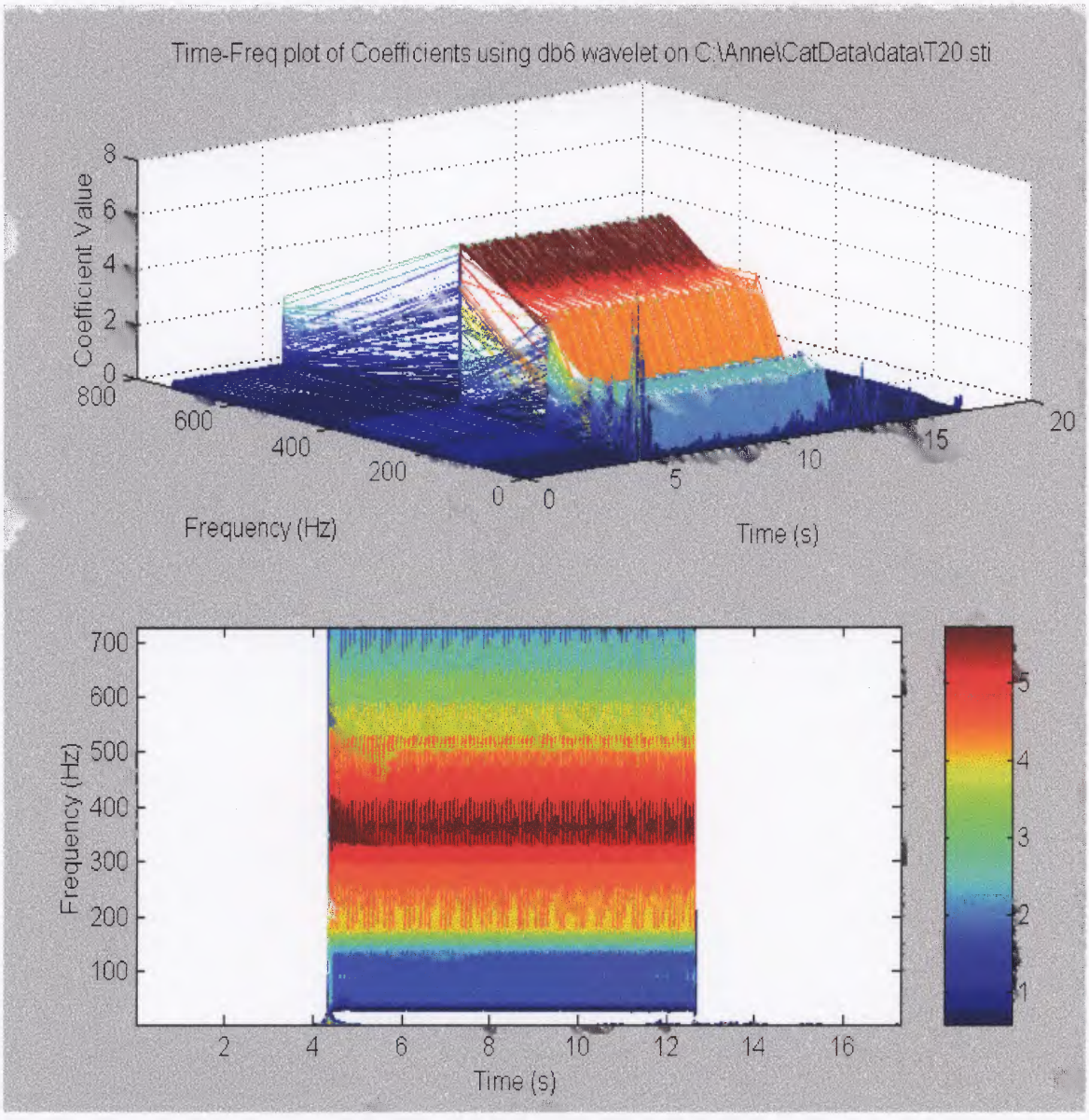

Figure 4.1 Continuous wavelet transform of EMG activity during Hypothalamic stimulation. Note the short lived, high power burst in low frequency activity at the onset of stimulation. The frequency activity in the 3-30 Hz range does not possess power comparable to that seen in the 300-400 Hz frequency range. This supports the observation in Section 2.4.3 that the power in the stimulation files is concentrated at frequency levels higher than those observed in the mastication files.

stimulation files, but the presence of this component is more easily detected in the mastication files than in the stimulation files.

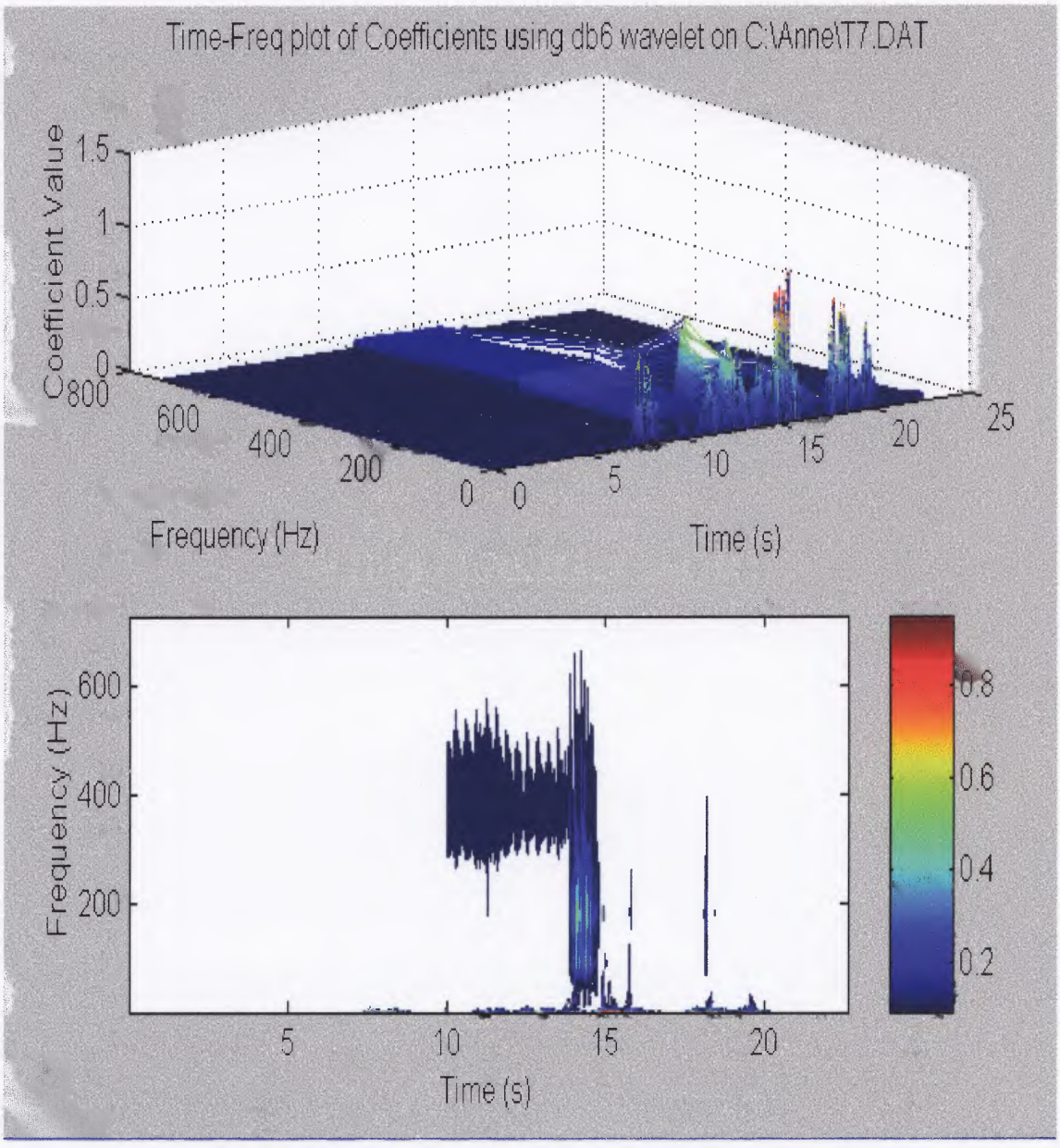

Figure 4.2 Continuous wavelet transform of EMG activity during Mastication. Note the downward shift in frequency activity from 300-500 Hz to the 75-200 Hz range. The high power activity is located in the 3-30 Hz range, as the mean power frequency analysis in Section 2.4.3 indicated.

As can be seen in Figure 4.1, there is a high power component in the frequency range of 3-30 Hz at the onset of stimulation. This activity then disappears until the last 25% of the stimulation period, when activity is again detected in the 3-15 Hz range. This component is present at a very low power in proportion to the rest of the frequency activity that is occurring during stimulation. High power frequency components remain present in this low frequency band well after the activity ends in both the stimulation and mastication files.

The power of the coefficients is significantly higher at all frequencies in the stimulation files than in the mastication files. The frequency and power content of the mastication signal vary over the course of the mastication signal. In contrast, the power and frequency content of the EMG signal during the stimulation period remain fairly consistent in power across all frequency ranges. The mastication files, which simulate voluntary masseter activity, displayed a high frequency content (300-500 Hz) upon commencement of the activity. In these recordings, the power of the EMG signal shifted down to the 75-200 Hz frequency band approximately two-thirds of the way into the mastication activity. In contrast, the emotionally-mediated EMG activity maintained a relatively constant, high power content in the 300-500 Hz frequency range throughout the duration of the recording. One stimulation file out of 22 displayed power levels higher than the other stimulation files. However, the characteristic stimulation frequency pattern that is seen in all stimulation files is present in this file, as well. The plot of this file, Figure 4.3, is above. Note that the magnitude for the typical stimulation file ranges from 0 to 5, and that this magnitude ranges from 0 to 20.

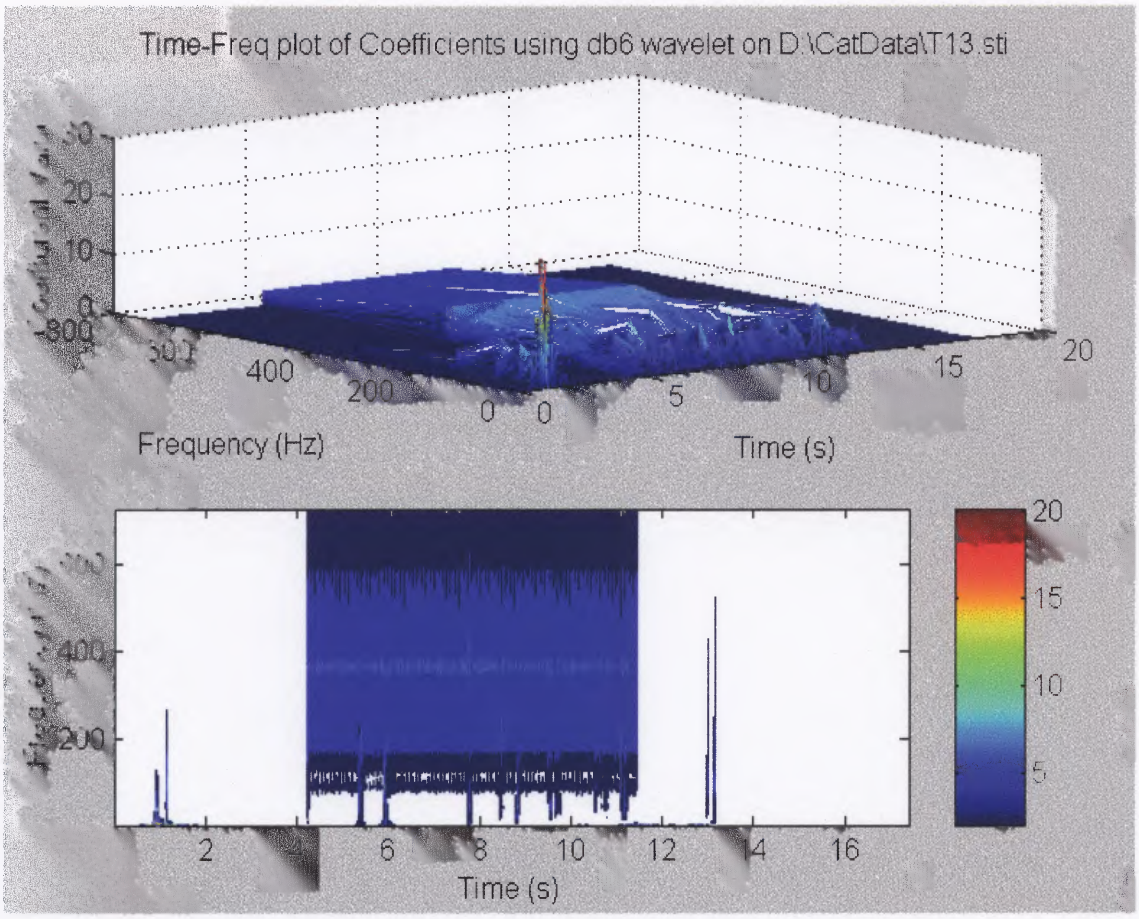

Figure 4.3 Stimulation file. Power levels are higher than other stimulation files, but data display similar frequency trends. Note that the magnitudes range from 0 to 20.

In an effort to quantify the changes that are observable via visible analysis for purposes of statistical quantification, the results were tabulated in terms of scale. The mean value and area under the curve at each scale, for each signal, throughout the duration of the signal, is tabulated and analyzed. The results are presented in Tables 4.3 through 4.8.

The results of this research are presented in terms of both scale and frequency, although the analysis in terms of scales is the basis for the results. Therefore, it is appropriate to indicate how the frequency translates to scale for the specific wavelet used in this research, the DauBechies, order 6 wavelet. Table 4.2 translates the Scale values to

Frequency values. Scale was defined and appropriate equations and relations to frequency are detailed in Chapter 3. Note that with increasing scale, the frequency decreases. The data in this chapter are plotted in terms of increasing scale, or decreasing frequency.

Table 4.2 Approximate Translation of Scale to Frequency Values

Scale	Frequency [Hz]
1	364 – 727
2	182 – 364
3	91 – 182
4	45 – 91
5	23 – 45
6	11 – 23
7	6 – 11
8	3 – 6

4.2.2 Scale Analysis of CWT Coefficients

The individual subject data during mastication for mean values per scale is included in Table 4.3. Table 4.4 provides the areas under the curve on a per scale basis of the mastication data. Table 4.5 details the mean values on a per scale basis for emotionally-mediated muscle activity. Table 4.6 provides the areas under the curve on a per scale basis for the stimulation data obtained in this study. The two animals had different responses to the stimulation, as is reflected in the magnitudes of the mean and area of the stimulation files versus the magnitudes calculated from the mastication files, as can be seen in the tables. The mastication files indicate that the magnitude of the reaction in the masseter muscle was similar for both animals. The results from the stimulation files indicate that there was a difference in reaction between animals to the stimulation (refer to Tables 4.5 and 4.6). Some scales indicate a difference of an order of six between the animals for the mean and area parameters. However, regardless of inter-animal

differences, the differences between behavioral states were highly significant in all scales, for both the mean and area parameters. Also note that in Tables 4.3 and 4.4 there is no significant difference between the responses of the animals during mastication.

Table 4.3 Mean Value of Individual Mastication Files, on a per Scale Basis

File	Scale 1	Scale 2	Scale 3	Scale 4	Scale 5	Scale 6	Scale 7	Scale 8
L1.dat	0.1453	0.2283	0.3688	0.3651	0.1614	0.2045	0.4422	0.6938
L10.dat	0.1185	0.419	0.5794	0.5831	0.2056	0.2695	0.3199	0.7698
L12.dat	0.0916	0.4572	0.6243	0.5082	0.3331	0.3216	0.3622	0.5747
L15.dat	0.1086	0.3318	0.5469	0.5415	0.2407	0.3294	0.4812	0.7386
L16.dat	0.5794	0.4205	0.4209	0.438	0.2488	0.1559	0.4246	0.5471
L18.dat	0.2522	0.35	0.5165	0.3989	0.2071	0.1729	0.2616	0.5012
L19.dat	0.0876	0.2114	0.548	0.4058	0.2132	0.1375	0.1304	0.351
L20.dat	0.2372	0.3602	0.4797	0.3586	0.1584	0.1262	0.1672	0.4531
L3.dat	0.0936	0.1852	0.5144	0.4064	0.1461	0.132	0.2772	0.6698
L5.dat	0.099	0.2183	0.4681	0.3847	0.1575	0.2802	0.2541	0.5773
L6.dat	0.1366	0.3244	0.7127	0.5241	0.3149	0.2014	0.5008	0.738
T1.dat	0.0581	0.2358	0.5138	0.4455	0.1915	0.1928	0.2688	0.8351
T10.dat	0.0752	0.2769	0.5766	0.4565	0.2563	0.2615	0.1964	0.6167
T11.dat	0.1131	0.2798	0.7482	0.5401	0.2053	0.234	0.2021	0.5457
T12.dat	0.0636	0.2541	0.5903	0.5153	0.1852	0.1802	0.2392	0.5289
T15.dat	0.067	0.2193	0.6244	0.4099	0.1531	0.2483	0.2273	0.5629
T16.dat	0.0641	0.2899	0.6393	0.5287	0.2127	0.2008	0.3208	0.6359
T3.dat	0.0715	0.2704	0.7746	0.716	0.2337	0.2232	0.2395	0.4726
T4.dat	0.1208	0.3449	0.6631	0.6139	0.268	0.2086	0.3156	0.8842
T6.dat	0.0603	0.2056	0.4254	0.3886	0.1852	0.3307	0.6683	1.0034
T7.dat	0.0589	0.253	0.5351	0.5209	0.1797	0.2648	0.2731	0.5084
T9.dat	0.0702	0.2312	0.5738	0.42	0.1505	0.1765	0.1906	0.5451

Table 4.4 Area Under the Curve for Mastication Files, on a per Scale Basis
Note that the values in the table are $*10^4$

File	Scale 1	Scale 2	Scale 3	Scale 4	Scale 5	Scale 6	Scale 7	Scale 8
L1.dat	0.52	0.81	1.31	1.30	0.58	0.73	1.58	2.47
L10.dat	0.52	1.84	2.55	2.57	0.90	1.19	1.41	3.39
L12.dat	0.42	2.10	2.87	2.33	1.53	1.48	1.66	2.64
L15.dat	0.49	1.49	2.46	2.43	1.08	1.48	2.16	3.32
L16.dat	2.57	1.86	1.86	1.94	1.10	0.69	1.88	2.42
L18.dat	1.09	1.51	2.23	1.72	0.89	0.75	1.13	2.17
L19.dat	0.39	0.93	2.42	1.79	0.94	0.61	0.58	1.55
L20.dat	0.97	1.47	1.95	1.46	0.65	0.51	0.68	1.85
L3.dat	0.36	0.72	1.99	1.57	0.56	0.51	1.07	2.59
L5.dat	0.40	0.89	1.91	1.57	0.64	1.14	1.04	2.35
L6.dat	0.63	1.49	3.26	2.40	1.44	0.92	2.29	3.38
T1.dat	0.16	0.63	1.37	1.19	0.51	0.52	0.72	2.23
T10.dat	0.33	1.22	2.53	2.01	1.13	1.15	0.86	2.71
T11.dat	0.47	1.15	3.08	2.23	0.85	0.96	0.83	2.25
T12.dat	0.29	1.17	2.72	2.37	0.85	0.83	1.10	2.43
T13.dat	0.28	0.91	2.59	1.70	0.64	1.03	0.94	2.34
T16.dat	0.26	1.17	2.57	2.13	0.86	0.81	1.29	2.56
T3.dat	0.22	0.84	2.40	2.22	0.72	0.69	0.74	1.46
T4.dat	0.37	1.05	2.03	1.88	0.82	0.64	0.96	2.70
T6.dat	0.14	0.48	1.00	0.91	0.44	0.78	1.57	2.36
T7.dat	0.27	1.14	2.42	2.36	0.81	1.20	1.24	2.30
T9.dat	0.28	0.92	2.29	1.68	0.60	0.71	0.76	2.18

Table 4.5 Mean Value of Individual Stimulation Files, on a per Scale Basis

File	Scale 1	Scale 2	Scale 3	Scale 4	Scale 5	Scale 6	Scale 7	Scale 8
L1.sti	0.9025	1.5243	1.3566	0.6193	0.2634	0.4487	0.4146	1.0256
L10.sti	0.7371	1.3913	1.11	0.6176	0.24	0.3002	0.4241	0.8947
L11.sti	0.7771	1.2504	1.0197	0.6141	0.2295	0.3851	0.6581	0.8499
L13.sti	0.8197	1.21	1.1362	0.5458	0.2233	0.2772	0.5371	0.9319
L15.sti	0.7964	1.2196	1.0771	0.5092	0.2167	0.2906	0.4389	0.6536
L17.sti	0.8561	1.2586	1.0672	0.6471	0.2184	0.2838	0.4501	0.9186
L18.sti	0.8989	1.2748	1.1781	0.6122	0.3666	0.4814	0.3812	0.6046
L20.sti	0.746	1.1925	1.0237	0.7232	0.3177	0.366	0.2362	0.2624
L22.sti	0.7478	1.1432	1.0591	0.5968	0.3308	0.3861	0.3152	0.6836
L24.sti	0.8203	1.1328	0.9321	0.5787	0.178	0.1909	0.273	0.6572
L4.sti	0.7733	1.1912	0.9651	0.5936	0.4155	0.298	0.5023	0.9592
T12.sti	2.7322	6.4249	4.8187	3.2329	1.9311	1.2837	1.369	1.0953
T13.sti	2.8175	7.1112	6.9129	8.2489	7.4684	5.9289	6.9845	14.733
T15.sti	2.7271	6.3346	5.0235	3.0826	2.4363	1.6292	1.4355	1.2964
T16.sti	2.7363	6.3039	4.7946	3.8096	2.6101	1.6099	1.2899	3.433
T18.sti	2.741	6.3071	4.8177	4.3583	8.0041	7.7454	3.7576	1.8636
T2.sti	2.7608	6.3525	4.6214	2.9877	2.2766	2.2428	2.1404	1.7281
T3.sti	2.771	6.2776	4.8882	4.0055	2.1668	0.6256	1.6966	2.8736
T4.sti	2.7499	6.2846	4.7747	3.1798	2.2683	2.2156	3.3814	2.6021
T6.sti	2.7386	6.309	4.8158	3.2869	1.8963	0.6961	0.9183	1.0271
T7.sti	2.7357	6.2944	4.7783	3.8713	2.0411	1.7136	1.7163	4.241
T8.sti	2.7318	6.3243	4.7615	2.7987	1.9147	1.5831	1.6702	4.3571

Table 4.6 Area Under the Curve for Stimulation Files, on a per Scale Basis
Note that the values in the table are $*10^4$

File	Scale 1	Scale 2	Scale 3	Scale 4	Scale 5	Scale 6	Scale 7	Scale 8
L1.sti	3.69	6.23	5.55	2.53	1.08	1.84	1.70	4.20
L10.sti	3.16	5.95	4.75	2.64	1.03	1.28	1.82	3.83
L11.sti	3.43	5.52	4.50	2.71	1.01	1.70	2.91	3.75
L13.sti	3.64	5.38	5.05	2.43	0.99	1.23	2.39	4.14
L15.sti	3.56	5.45	4.81	2.28	0.97	1.30	1.96	2.92
L17.sti	3.39	4.99	4.23	2.57	0.87	1.13	1.78	3.64
L18.sti	3.79	5.37	4.97	2.58	1.55	2.03	1.61	2.55
L20.sti	3.17	5.06	4.35	3.07	1.35	1.55	1.00	1.11
L22.sti	3.07	4.70	4.35	2.45	1.36	1.59	1.30	2.81
L24.sti	3.46	4.78	3.93	2.44	0.75	0.81	1.15	2.77
L4.sti	3.69	5.69	4.61	2.83	1.98	1.42	2.40	4.58
T12.sti	9.48	22.30	16.72	11.22	6.70	4.45	4.75	3.80
T13.sti	9.81	24.75	24.06	28.71	25.99	20.63	24.31	5.13
T15.sti	10.42	24.20	19.19	11.78	9.31	6.22	5.48	4.95
T16.sti	10.75	24.78	18.84	14.97	10.26	6.33	5.07	13.49
T18.sti	9.54	21.95	16.77	15.17	27.86	26.96	13.08	6.49
T2.sti	8.84	20.33	14.79	9.56	7.29	7.18	6.85	5.53
T20.sti	10.72	24.10	17.43	9.01	5.64	5.11	10.05	9.70
T3.sti	8.11	18.36	14.30	11.72	6.34	1.83	4.96	8.41
T4.sti	9.25	21.15	16.07	10.70	7.63	7.46	11.38	8.76
T6.sti	9.45	21.77	16.62	11.34	6.54	2.40	3.17	3.54
T7.sti	10.83	24.93	18.92	15.33	8.08	6.79	6.80	16.80
T8.sti	10.03	23.21	17.48	10.27	7.03	5.81	6.13	15.99

Statistical analysis reveals significant differences in the mean value and area under the curve at each scale. Since the analysis is investigating the differences in EMG response in the same animal between two different behavioral states, a paired t-test is

appropriate. The intent of this test is to determine whether the values are the same for the behavioral states being investigated. The null hypothesis, which is what the research is attempting to disprove, states that there is no difference between the values obtained during simulated mastication, which represents the voluntary masseter activity, and the hypothalamically stimulated activity, which gives an indication of masseter activity during stress. The tests used a 0.05 level of significance, which means that there is less than a 5% chance that the test would reject the null hypothesis if it was true.

There are highly significant differences between values obtained during stimulation and those obtained during mastication (Tables 4.7 and 4.8). This statement is supported by the fact that the probability that the t-value is less than the t-statistic ($P(T \leq t)$) for all scales was less than 0.05, as can be seen in Tables 4.7 and 4.8. Probabilities ($P(T \leq t)$) less than 0.05 suggest that the mean values for the different behavioral states are significantly different, and the differences cannot be attributed to a sampling error. A probability less than 0.01 indicates that the difference is highly significant [29]. In this case, all values are less than 0.01.

Table 4.7 Statistical Values of Mean of Mastication and Stimulation Data

Scale	Mean – Mast	Mean - Stim	Stim/Mast ratio	Var - Mast	Var – Stim	Stim/ Mast ratio	# Obs	P(T<=t) two-tail
1	0.13	1.77	14.08	0.01	0.98	75.65	22	0.00000030
2	0.29	3.79	13.08	0.01	6.73	1139.08	22	0.00000337
3	0.57	2.99	5.29	0.01	3.86	356.65	22	0.00000747
4	0.48	2.00	4.21	0.01	2.13	256.22	22	0.00005782
5	0.21	1.21	5.76	0.00	0.94	354.73	22	0.00010251
6	0.22	0.90	4.08	0.00	0.47	123.92	22	0.00015787
7	0.31	1.06	3.44	0.02	0.63	38.24	22	0.00034163
8	0.63	1.58	2.52	0.02	1.43	59.81	22	0.00151030

Table 4.8 Statistical Values of Area of Mastication and Stimulation Data

Scale	Mean – Mast	Mean - Stim	Stim/Mast ratio	Var - Mast	Var - Stim	Stim/Mast ratio	# Samples	P(T<=t) two-tail
1	0.52	6.63	12.78	0.26	10.90	41.46	22	0.00000008
2	1.17	13.98	11.92	0.18	79.72	453.65	22	0.00000164
3	2.26	11.09	4.90	0.31	45.74	147.69	22	0.00000483
4	1.90	7.38	3.89	0.20	25.79	127.68	22	0.00005665
5	0.84	4.42	5.25	0.08	11.76	147.78	22	0.00010858
6	0.88	3.35	3.82	0.08	5.64	66.60	22	0.00009458
7	1.20	3.90	3.24	0.23	6.81	29.48	22	0.00021227
8	2.44	5.96	2.44	0.24	18.90	77.25	22	0.00140519

4.2.3 Significance and Ratios of Stimulation to Mastication

The mean value of each scale is significantly larger in the stimulation files than in the mastication files, as is the area of each scale. The significance of the difference between mastication and stimulation increases as the frequency increases, as seen in Figure 4.4, for both mean scale value and area under the curve for each scale. This indicates that the emotional component of the EMG activity is more significant in the fast fatiguing muscle fibers than in slow fatiguing muscle fibers.

The ratios of the power in the stimulation/mastication values of area and mean per scale vary similarly across the entire frequency range, as can be seen in Figure 4.5. This variation indicates that the ratios decrease as the frequency decreases. This indicates that as the frequency decreases, the values of the stimulation and mastication files become more similar, although the stimulation files maintain a significantly higher magnitude

than the mastication files. Just as with the variations in significance parameters, this indicates that the emotional component may be more powerful in the modulation of the recruitment of fast firing, fast fatiguing muscles than the voluntary component. It also may indicate that the lower frequency, slower fatiguing muscle fibers may be more equally influenced by voluntary and emotionally-mediated activity than are fast firing muscle fibers.

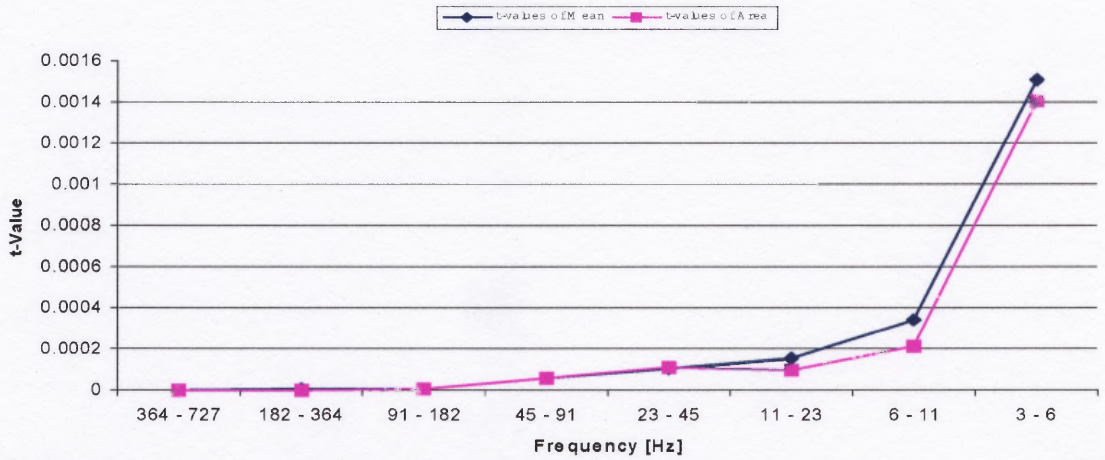

Figure 4.4 t-Value trends. Note the lower frequencies are at the right hand side of the plot.

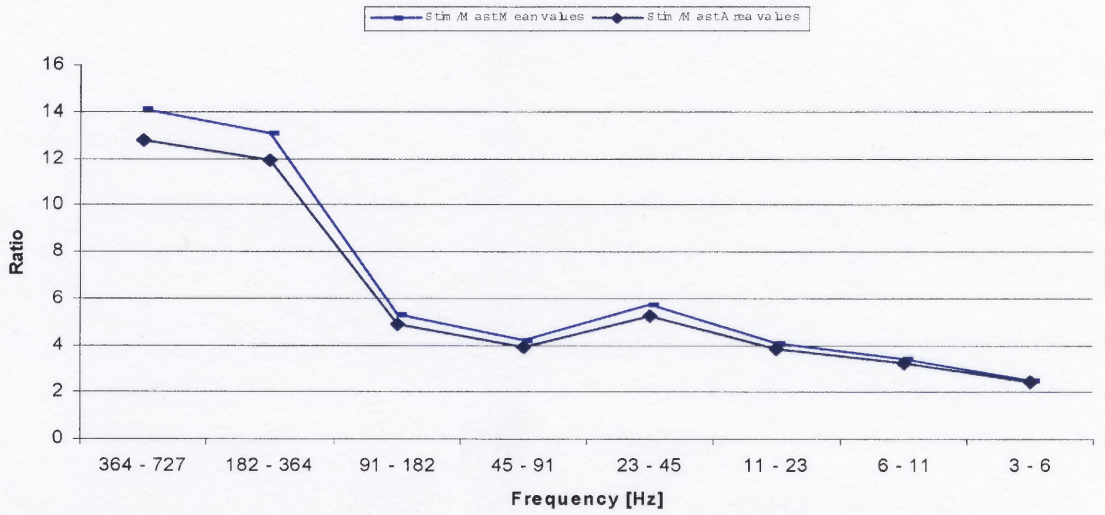

Figure 4.5 Stimulation/Mastication Ratios for the area and mean value parameters.

4.3 Discussion of Results

Muscle hyperactivity in patients suffering from a temporomandibular joint disorder may be associated with emotional stressors. The paired symptomology of jaw pain and stiffness resulting from stressors may be associated with an initial elevated level of EMG activity. In this animal model, the emotional stress was initiated from the hypothalamus directly by electrical stimulation. Thus, at other intervals there would be little residual emotional response present. If this was a study done with humans for whom stress responses are of long duration, the data might be even more compelling. However, this animal model illustrates that during emotionally-mediated EMG activity, the magnitude of the EMG response is significantly elevated relative to the EMG response during mastication. There is also no variation in the power or frequency of the EMG activity, while the mastication data show variations in both the frequency and power levels of the EMG activity.

One question that has been addressed in this research is whether the increased EMG response is associated with an increase in the recruitment of fast firing muscle fibers during stressful activity or if there was a shift in the frequency of the firing of the fibers. The former scenario would be validated if the power of the frequency content was elevated during the signal. Higher power would indicate that more muscle fibers are being recruited at that given frequency. The latter situation would be validated if the power of the EMG signal remained fairly constant throughout the course of the experiment, but the frequency content at which the main power is located would change. Studies on fatigue have indicated that the proportion of signal power shifts from higher to lower frequencies when fatigue occurs [11, 30, 31]. Thus, during fatigue the fibers fire

less frequently, but with the same power. In this series of experiments, it was observed that the mastication data displayed this shifting pattern of frequency content. The wavelet time frequency representation that captures this shift is clearly displayed in Figure 4.2. During emotionally-mediated EMG activity, however, this downward frequency shift is not present, as can be observed in Figure 4.1. Combining this observation with the elevated power in the high frequency range, it indicates that even when fatigue should set in and cause muscle recruitment modulation, which activates slower firing fibers during fatigue, this safety mechanism does not commence. Instead, the fast fatiguing muscle fibers remain active throughout the period of stimulation, with no evident modulation.

This research also indicates that there is a significant high frequency component that is present during emotional display that is absent during mastication. The frequency content of the EMG signal during both types of behavioral activity begins in the same frequency range, although the stimulation data possess greater power in the frequency band. With time, the mastication files typically display a pattern of shifting to lower frequency ranges, perhaps indicative of the recruitment of slow fatiguing motor units. This may also be indicative of some central control activity occurring. The lower power, high frequency content remains present when the shift occurs. However, the peak power shifts from between 300 and 500 Hz to between 100 and 200 Hz during mastication. The power remains concentrated between 300 and 500 Hz during the stimulated EMG activity. At the end of the stimulation period, a short duration low power frequency band is seen between 100 and 300 Hz. This suggests that emotionally-mediated muscle activity does not demonstrate a typical muscle recruitment pattern, but instead recruits

larger numbers of fast fatiguing muscle fibers for extended periods of time by bypassing muscle feedback mechanisms. The protective mechanisms that would recruit slow fatiguing motor units are apparently over-ridden during emotional behavior and may be associated with the muscular pain that is concurrent with TMD.

There is a low frequency component at approximately 10 to 30 Hz that has a signature trace that differs for both the stimulation and mastication files. During mastication, this signal is present throughout the duration of the muscle activity, with bursts of EMG activity occurring after the main mastication activity has ended, as is seen in Figure 4.1. The post-activity bursts are apparent in the stimulation files (refer to Figure 4.2), as well, but there is a more significant amount of time between the bursts in the stimulation files than in the mastication files. While the mastication files contain this low frequency content throughout the duration of the signal, the stimulation files display this activity only in the last 0.25% of the stimulation period. The origins of this low frequency content are unclear, although as indicated in Section 4.3, the low frequency content between 5 and 30 Hz may be an indication of fatigue. It seems unlikely that this can be a reliable indicator of fatigue during stimulation due to the high power content in this frequency range at the onset of the stimulation during the recordings. It is also possible that the bursts occurring after the activity has ceased may be residual cortical evoked potential associated with EMG activity. This low frequency content should be investigated further in future studies. It may well provide a signature for EMG activity resulting from varying behavioral patterns, casting more light on signals that control muscle activity.

This research expands the previous findings that demonstrated elevations in mean power frequency (MPF) and raw EMG values, as well as changes in median frequency [1, 16, 17]. Previously, the contributing factors in the elevated MPF during stimulation were unclear. It was unclear whether the elevation was a result of increased power at specific points in time or whether there were certain components present throughout the duration of the signal. This study identified the various frequency components present at specific points in time of the signal (refer to Section 4.2.1) during the two behavioral states. It also identified metrics that suggest that emotional input is more significant at higher frequencies than at lower frequencies. In addition, this research proves that the wavelet time frequency decomposition is well suited to yielding the time resolution that has been previously unavailable in studies of this nature.

CHAPTER 5

CONCLUSION AND SUGGESTIONS FOR FUTURE RESEARCH

A summary of the results of this research and recommendations for future work will be the focus of this chapter.

5.1 Summary of Results

This work substantiates several important conclusions regarding muscle activity that occurs during voluntary versus emotionally-mediated behavioral states. A major observation is that the values of the power of the wavelet coefficients are significantly higher in all frequency ranges for stimulation files than for mastication files. This would indicate that a more extensive recruitment of fast firing motor neurons occurs when an emotional component is present. This clarifies previous studies, which noted increased mean power frequency, but could not specify whether this was the result of a higher number of neurons firing or whether there was a shift in the frequency of the motor neurons which are recruited. This study indicates that the shift in frequency content from high to low that occurs during voluntary masseter activation is not present in the activity that is recorded during hypothalamically stimulated muscle activity.

Another observation is that the significance of the difference between the values in the mastication and stimulation files increases as the frequency increases. It also is noted that the magnitude of the coefficients increases more rapidly in the stimulation files than in the mastication files as the frequency increases. This would indicate that the high frequency component present during emotional stimulation is far more marked than

during mastication. This may indicate that the high frequency content is more significant during emotional stimulation than during voluntary activity, thus influencing the activity of the fast-firing motoneurons more substantially. It also indicates that emotionally mediated masseter activity calls upon a larger quantity of fast-firing, fast-fatiguing muscle fibers than the voluntary activity.

This study proves that the wavelet time frequency signal decomposition, using the DauBechies order 6 (db6) wavelet, is capable of delineating activity at various frequency levels and at the same time maintaining the time resolution that casts the most light on this data. It yields good time and frequency resolution. This method has already been demonstrated in other areas of EMG analysis, mainly in fatigue analysis. However, it has not been demonstrated in this type of model for distinguishing between hypothalamically induced behavioral patterns versus masseter muscle activity during voluntary behavioral states, such as mastication. This research illustrates the potential for further defining the role that stress plays in mediating muscle response in the temporomandibular joint using the wavelet time-frequency decomposition.

5.2 Suggestions for Future Work

This research provides a strong basis for future work using wavelet analysis techniques to clarify and further define the activity of the masseter muscle during different behavioral states. Future work should include a more thorough examination of the wavelet coefficients obtained in the decomposition of these data. This may be accomplished through means including, but not limited to, polynomial regression, slope analyses and wavelet modulus maxima and minima determinations. Wavelet modulus maxima and

minima indicate changes in frequency content above a specific threshold over the time of the signal. This type of analysis has been used in past studies to mark the specific point when fatigue begins to occur in the muscle. It would be useful in future studies of this type because it would provide a measurable index of frequency changes at various points in the life of the signal.

A difficulty in analyzing data of this nature is that the EMG activity does not occur at the same time in every data file. This confounds data analysis in the respect that with the time resolution that the wavelet analysis provides, it is not possible to compare the results due to differences in time of activation. The time of initiation and completion of muscle activity should be controlled more tightly for use in any future time-frequency analyses.

Another area of concern with this particular assessment of emotional mediation of muscle recruitment is distinguishing between the stimulation and the EMG activity. Although the stimulation artifact was filtered out with the 60 Hz noise filter, it is unclear whether the stimulation had a direct impact on the muscle activity. The resultant patterns detected by the wavelet analysis of the stimulation files may be muscle activity based upon physiologic input as a result from hypothalamic stimulation. They may also be the result of electrical stimulation placed in the vicinity of the muscle. A more specific method of separating the muscle activity from the stimulation signal would be appropriate in future studies. It may also be appropriate to perform a comparison between the EMG of muscle during hypothalamic stimulation versus masseteric EMG during stimulation of cortical regions that are thought to initiate voluntary movements. This may reduce the confusion regarding stimulation artifact that haunts research in this

area by providing a platform for comparing EMG activity during two stimulated behavioral states, rather than during one stimulated state and one simulated state.

The creation of an EMG specific wavelet might also aid in further clarifying the results of this research. The results of a wavelet analysis are only as good as the match of the signal shape to the shape of the mother wavelet [32]. While the DauBechies 6 wavelet provided a good approximation to the EMG signal shape, it is not the best approximation. Designing a wavelet specific to the shape of the EMG would enable the best accuracy of the wavelet coefficients for analysis. Recall that the coefficients are a measure of the correlation at various frequencies and times between the signal and the mother wavelet. If the coefficients are the basis for analysis, it is important that they be as accurate as possible. For purposes of reconstruction, any wavelet capable of performing a discrete wavelet transform is appropriate. However, for analysis of the frequency content of a signal, it is appropriate to demand the higher level of accuracy provided by a wavelet designed specifically for the signal that is to be analyzed.

It would be helpful to clarify activity that was observed in the 3-30 Hz frequency range, as well as to delineate artifact from other biological systems interfering with the EMG data obtained. To this end, it is suggested that concurrent measurements of Electroencephalogram (EEG) and Electrocardiogram (ECG) are recorded with the EMG signals. It is possible that studies of the EEG signal or heart rate variability may clarify the extent of activity in the branches in the Autonomic Nervous system during various behavioral states.

It is also recommended that a marker system be developed to indicate in the data files when events, such as eye blinking or movement of the head or jaw, occur during the

experiment. This would allow the researcher to properly identify motion artifact in the data. This may be implemented using a button push marker system, with specific codes inserted into the data for various activities. A camera system may also be implemented effectively to coordinate movements with data recordings.

It may be of interest to correlate force of jaw contraction with the power in various frequency bands during EMG activity. This may be accomplished with a force plate placed unilaterally in the animal's mouth. This correlation may aid in the further delineation of interplay between muscle fibers and the neural activity at the root of motor unit recruitment.

APPENDIX A

LABVIEW PROGRAM EMPLOYED IN THE RESEARCH

This Appendix contains the front and wiring panels of the Labview program used to filter the Data before performing the Wavelet analysis. The program performed bandpass filtering to remove DC content, as well as ensured that the highest frequency content contained within the signal is 750 Hz. It also notch filtered the data to remove any 60 Hz and stimulation artifact.

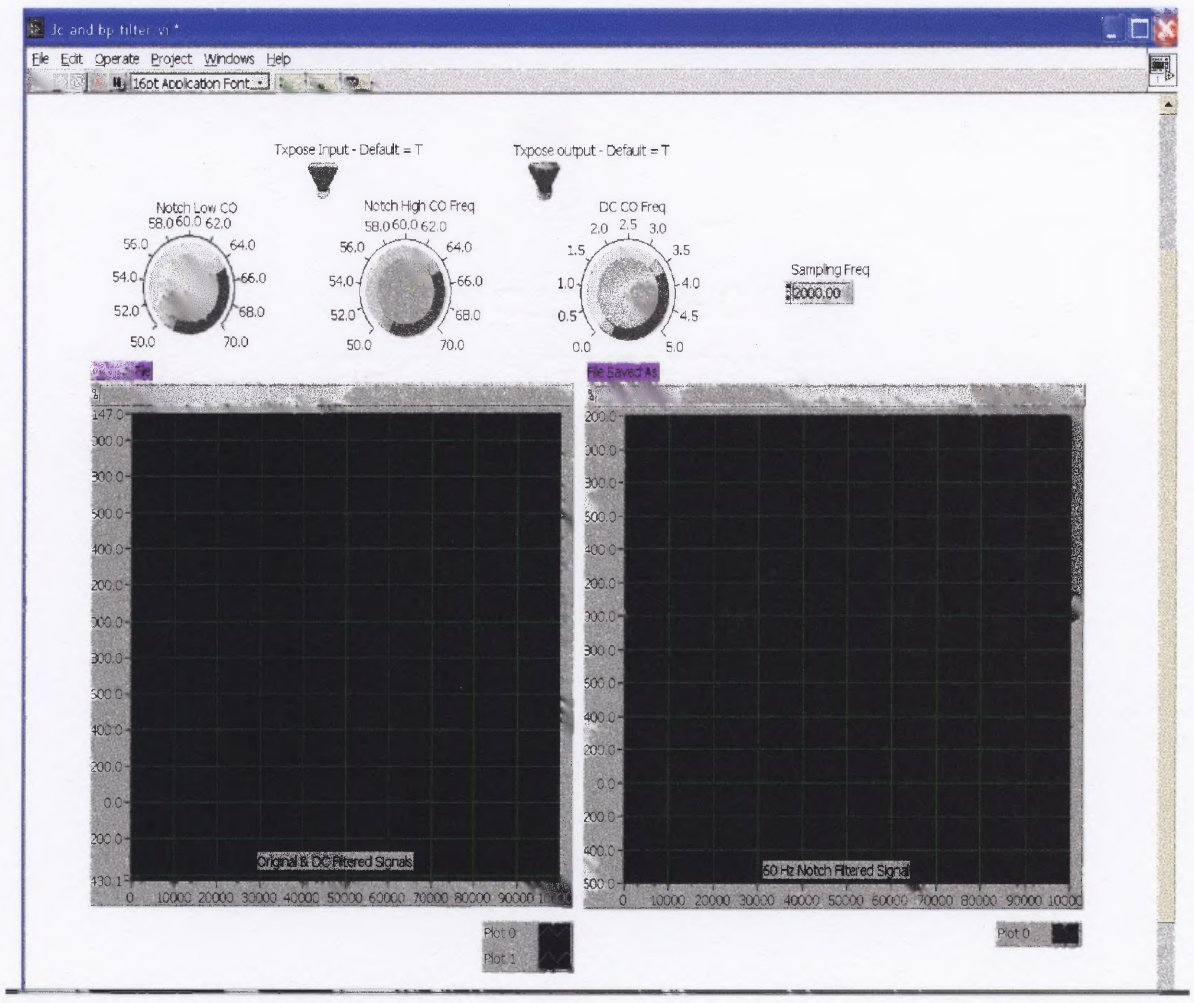

Figure A.1. Labview Front Panel.

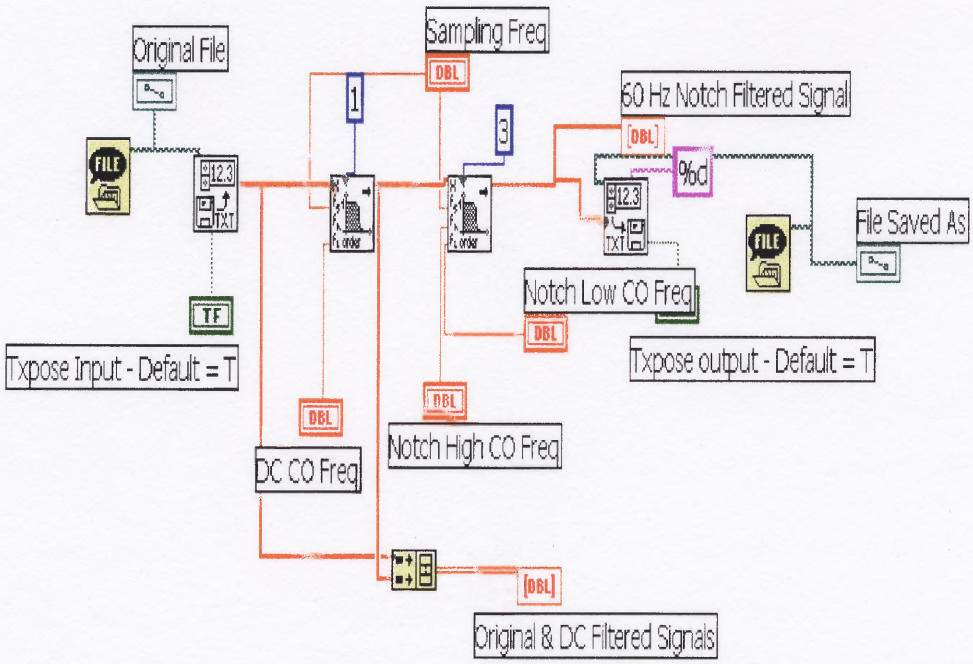

Figure A.2. Back panel of Labview program. The two filters are set to band pass and notch filter the data, as indicated by the order of the filter being 1 and 3, respectively.

APPENDIX B

MATLAB PROGRAM EMPLOYED IN THE RESEARCH

This Appendix contains the Matlab program that performed the wavelet analysis used in this research. This program takes user inputs of 'file to be analyzed' and 'wavelet type to use' and performs the discrete and continuous wavelet transforms on the file. The discrete analysis is performed to assess reconstruction capability. The continuous transform is performed to assess frequency activity throughout the duration of the signal. The program then outputs plots similar to 4.1 and 4.2, which are the three dimensional plots of the CWT coefficients. It outputs plots of the original and reconstructed signals, using the DWT. In addition, it generates plots of the individual detail and approximation signals for more detailed analyses of frequency components.

```
% This program will use the Matlab toolikit to perform a wavelet analysis on EMG
signals.
%This file will request which Wavelet Decomposition to perform.
% Using this information, it will decompose the signal and reconstruct it, saving
% the coefficient information obtained over the course of the analysis. It will
% then send the coefficients and reconstructed signal to a user-specified file and
% plot the original vs. reconstructed signals. It will also plot the T-F plot of the
% coefficients.
% Created by AM Petrock 11/20/2001.
% Modified 6/20/2002 to perform coefficient manipulation.

clear all;
clc;

% Ask the user to select the signal that is to be analyzed.
[fname,pname]=uigetfile('*.*','Please select the file that will be analyzed with a
wavelet:');

if isstr(fname) == 0
        disp(' Cannot find file')
        dbquit
```

```
end

Filename = [pname fname];
load(Filename) ;                % load file
fname = strtok(fname,'.');      % drop extension
k=eval(fname);                          % evaluate fname
signal=k(1000:length(k)); %Filter transient lasts approximately first 1000 points
N=length(signal);
ss=signal;
maxscale=8;     % Set max scale level, based on decomposition
ss = detrend(ss);

% Allow user to enter type of wavelet to be used in this analysis, accepting wave name as
'wn', a string.
wave=input('Please enter name of Wavelet to be used in analysis --->  ','s');

% Perform Discrete Wavelet decomposition using wavelet specified by user in the
beginning of this program. Decomposition is preformed at level 6,
% which approximates a scale level of 2^8, or 256.

[C,L]=wavedec(ss,maxscale, wave);

% Determine coefficients for Details and Approximations from Discrete Decomposition.
cA8=appcoef(C,L, wave,maxscale);
cD8=detcoef(C,L,maxscale);
cD7=detcoef(C,L,7);
cD6=detcoef(C,L,6);
cD5=detcoef(C,L,5);
cD4=detcoef(C,L,4);
cD3=detcoef(C,L,3);
cD2=detcoef(C,L,2);
cD1=detcoef(C,L,1);

% Perform Continuous Wavelet Transform

sf=2000;       % Sampling Freq for EMG signals is 2 kHz.
sp=1/sf;       % Sampling Period
a=2.^[1:maxscale];  % Set Scales
t=sp.*[1:length(ss)]; % convert file to seconds, not sample number
figure;  plot(t,ss)

% Compute CWT
sscwt=cwt(ss,a,wave);

% Compute pseudofrequencies
f=scal2frq(a, wave,sp);
```

```
% Compute pseudo-periods
per=1./f;

% Plot the CWT values in T-F
figure;
subplot(2,1,1);
mesh(t,f,abs(sscwt));
title(['Time-Freq plot of Coefficients using ' wave ' wavelet on ' Filename])
xlabel('Time (s)');
ylabel('Frequency (Hz)');
zlabel('Coefficient Value');

subplot(2,1,2);
contour(t,f,abs(sscwt),10);
xlabel('Time (s)');
ylabel('Frequency (Hz)');
colormap('jet')
colorbar('vert')
%shading interp

% Detrend coefficient values
dt1 = detrend(sscwt(1,:));
dt2 = detrend(sscwt(2,:));
dt3 = detrend(sscwt(3,:));
dt4 = detrend(sscwt(4,:));
dt5 = detrend(sscwt(5,:));
dt6 = detrend(sscwt(6,:));
dt7 = detrend(sscwt(7,:));
dt8 = detrend(sscwt(8,:));
dt9 = detrend(sscwt(9,:));

% Shift data to zero for integration
min = min(transpose(sscwt));
sscwt1 = sscwt(1,:) + abs(min(1));
sscwt2 = sscwt(2,:) + abs(min(2));
sscwt3 = sscwt(3,:) + abs(min(3));
sscwt4 = sscwt(4,:) + abs(min(4));
sscwt5 = sscwt(5,:) + abs(min(5));
sscwt6 = sscwt(6,:) + abs(min(6));
sscwt7 = sscwt(7,:) + abs(min(7));
sscwt8 = sscwt(8,:) + abs(min(8));
sscwt9 = sscwt(9,:) + abs(min(9));

sscwt_shift = [sscwt1;sscwt2;sscwt3;sscwt4;sscwt5;sscwt6;sscwt7;sscwt8;sscwt9];
```

```
% Perform coefficient manipulations
sscwTX_shift = sscwt_shift .';
mean_sscwt = mean(sscwTX_shift)
[min,imin] = min(sscwTX_shift)
[max,imax] = max(sscwTX_shift)
area_sscwt = sum(sscwTX_shift)

% Save CWT coefficients to a file
%[newfile1,newpath1] = uiputfile('*.*','Enter file to save CWT coefficients to:');
%fname1 = [newpath1 newfile1];
%fprintf(fname1, '%12.8f\n', sscwt);

% Plot solid figure of coefficients in T-F domain.
%figure;
 %  surface(per, f, abs(sscwt));
  % [az,el]=view;
   %view(az,el);
   %xlabel('time');
   %ylabel('freqency');
   %title(['T-F Decomposition of ' ss ' using ' wave ' wavelet']);

% Reconstruct Details and Approximations.
A8=wrcoef('a',C,L, wave,8);
D8=wrcoef('d',C,L, wave,8);
D7=wrcoef('d',C,L, wave,7);
D6=wrcoef('d',C,L, wave,6);
D5=wrcoef('d',C,L, wave,5);
D4=wrcoef('d',C,L, wave,4);
D3=wrcoef('d',C,L, wave,3);
D2=wrcoef('d',C,L, wave,2);
D1=wrcoef('d',C,L, wave,1);
X=[A9 D9 D8 D7 D6 D5 D4 D3 D2 D1];

figure
subplot(2,1,1);plot(t,D1)
title(['Scale 2 (f= 727 Hz) value using ' wave ' wavelet on ' fname])
xlabel('Time (s)');
ylabel('Wavelet Coefficient')

subplot(2,1,2);plot(t,D2)
title(['Scale 4 (f= 364 Hz) value using ' wave ' Wavelet'])
xlabel('Time (s)');
ylabel('Wavelet Coefficient')


figure
```

```
subplot(2,1,1);plot(t,D3)
title(['Scale 8 (f = 182 Hz) value using ' wave ' wavelet on ' fname])
xlabel('Time (s)');
ylabel('Wavelet Coefficient')

subplot(2,1,2);plot(t,D4)
title(['Scale 16 (f = 91 Hz) value using ' wave ' Wavelet'])
xlabel('Time (s)');
ylabel('Wavelet Coefficient')


figure
subplot(2,1,1);plot(t,D5)
title(['Scale 32 (f = 46 Hz) value using ' wave ' Wavelet on ' fname])
xlabel('Time (s)');
ylabel('Wavelet Coefficient')

subplot(2,1,2);plot(t,D6)
title(['Scale 64 (f = 23 Hz) value using ' wave ' Wavelet'])
xlabel('Time (s)');
ylabel('Wavelet Coefficient')


figure
subplot(2,1,1);plot(t,D7)
title(['Scale 128 (f = 11 Hz) using ' wave ' Wavelet on ' fname])
xlabel('Time (s)');
ylabel('Wavelet Coefficient')

subplot(2,1,2);plot(t,D8)
title(['Scale 256 (f = 6 Hz) using ' wave ' Wavelet'])
xlabel('Time (s)');
ylabel('Wavelet Coefficient')


% Save Reconstructed Coefficient data to a file
%[newfile2,newpath2] = uiputfile('*.*','Enter file to save DWT coefficients to:');
%fname2 = [newpath2 newfile2];
%fprintf(fname2, '%12.8f\n', X);

% Reconstruct signal from coefficients:
A0=waverec(C,L, wave);

% Plot Original vs. Reconstructed Signals
figure
subplot(2,1,1); plot(t,ss); title(['Original Signal,  ' fname]);
```

```
subplot(2,1,2); plot(t,A0); title(['Reconstructed signal using ' wave ' wavelet decomposition']);

% Save reconstructed signal to a file
%[newfile3,newpath3] = uiputfile('*.*','Enter file to save recontructed signal to:');
%fname3 = [newpath3 newfile3];
%fprintf(fname3, '%12.8f\n', A0);
%fscanf reads the data from this file into an array
```

REFERENCES

[1] Weiner, S., Shaikh, M., and A. Siegel, "Electromyographic Activity in the Masseter Muscle Resulting from Stimulation of Hypothalamic Behavioral Sites in the Cat," *J. Orofacial Pain*. 1993; 7; 370-376.

[2] Bowen, R. The Hypothalamus and Pituitary Gland: Introduction and Index. http://arbl.cvmbs.colostate.edu/hbooks/pathphys/endocrine/hypopit/. (27 April 2002)

[3] Hypothalamus and Autonomic Nervous System. http://thalamus.wustl.edu/course/hypoAND.html. (27 April 2002)

[4] Hormones and stress: The pituitary-adrenal-axis in learning and memory. http://salmon.psy.plym.ac.uk/year1/stressho.htm. (27 April 2002)

[5] Temporomandibular Disorders (TMD). http://www.nidcr.nih.gov/health/pubs/tmd/menu.htm. (27 April 2002)

[6] Temporomandibular Disorders (TMD). http://www.nidcr.nih.gov/health/pubs/tmd/sec4.htm. (27 April 2002)

[7] Temporomandibular Disorders (TMD): What Causes TMD? http://www.nudcr.nih.gov/health/pubs/tmd/sec3.htm. (27 April 2002)

[8] Temporomandibular Disorders (TMD): What Are Temporomandibular Disorders? http://www.nudcr.nih.gov/health/pubs/tmd/sec3.htm. (27 April 2002)

[9] Petres, R., and S. Gross. *Temporomandibular Disorders and Orofacial Pain*, Chicago: Quintessence Publishing, 1995.

[10] Ottoson, D. *Physiology of the Nervous System*. New York: Oxford University Press, 1983.

[11] Sparto, P., Parnianpour, M., Barria, E. and J. Jagadeesh, "Wavelet and Short-Time Fourier Transform Analysis of Electromyography for Detection of Back Muscle Fatigue." *IEEE Trans. on Rehabilitation Engineering* 8:3 (2000): 433-36.

[12] Dolan, P., Mannion, A., and M. Adams. "Fatigue of the Erector Spinae Muscles. A Quantitative Assessment using "frequency banding" of the Surface Electromyography Signal." *Spine* 20 (1995): 149-159.

[13] Vander, A., Sherman, J. and D. Luciano. *Human Physiology: The Mechanisms of Body Function*. 5th Ed. New York: McGraw-Hill, 2001.

[14] Webster, J., ed. *Medical Instrumentation: Application and Design*. 3rd Ed. New York: John Wiley and Sons, 1998.

[15] Jasper, H., and C. Ajmone-Marson. *Stereotaxic Atlas of the Diencephalon of the Cat*. National Research Council of Canada, 1954.

[16] Smitthisomwong, P., Weiner, S., Levin, L., Reisman, S., and A. Siegel. "The Effect of a Cholecystokinin Agonist on Masseter Muscle Activity in the Cat." *J. Dental Research* 79:10 (2000): 1823-28.

[17] Hellstrom, F., Thunberg, J., Bergenheim, M., Sjolander, P., Pederson, J., and H. Johansson. "Elevated Intramuscular Concentration of Bradykinin in Jaw Muscle Increases the Fusimotor Drive to Neck Muscles in the Cat." *J. Dent. Res.* 79:10 (2000): 1815-22.

[18] Poularikas, A., ed. *Transforms and Applications Handbook*. London: CRC Press, January 1996.

[19] Mallat, S., *A Wavelet Tour of Signal Processing*. San Diego: Academic, 1998.

[20] Mathworks, Incorporated. *Matlab Wavelet Toolkit*. Rev. 2. http://www.mathworks.com/access/helpdesk/help/pdf_doc/wavelet/wavelet_ug.pdf. (September 2001)

[21] Serrano, E. and M. Fabio. "Application of Wavelet Transform to Acoustic Emission Signal Processing." *IEEE Trans. on Signal Processing* 44:5 (1996): 1270-75.

[22] Martin, N., Mars, J., Martin, J., and C. Chorier. "A Capon's Time-Octave Representation Application in Room Acoustics." *IEEE Trans. on Signal Processing* 43:8 (1995): 1842-54.

[23] Shang, L., Herold, G., and J. Jaeger. "A New Approach to High-Speed Protection for Transmission Line Based on Transient Signal Analysis Using Wavelets." *IEEE Developments in Power System Protection, Conference Publication* 479 (2001): 173-76.

[24] Maass, P., Tescheke, G., Willmann, W., and G. Wollmann. "Detection and Classification of Material Attributes – A Practical Application of Wavelet Analysis." *IEEE Trans. on Signal Processing* 48:8 (2000):2432-38.

[25] Pattichis, C., and M. Pattichis. "Time-Scale Analysis of Motor Unit Action Potentials." *IEEE Trans. on Biomedical Engineering* 46:11 (1999): 1320-29.

[26] National Instruments Corporation. *Wavelet and Filter Bank Design Toolkit Reference Manual*. January, 1997. http://www.ni.com/pdf/manuals/321380a.pdf. (February 2002)

[27] Valens, C. "A Really Friendly Guide to Wavelets." 1999. http://perso.wanadoo.fr/polyvalens/clemens/wavelets/wavelets.html. (August 2002)

[28] Karlsson, J., Gerdle, B., and M. Akay. "Analyzing Surface Myoelectric Signals Recorded During Isokinetic Contractions." *IEEE Engineering In Medicine and Biology* 6 (2001): 97-105.

[29] Mezei, L. *Practical Spreadsheet Statitstics and Curve Fitting for Scientists and Engineers.* New Jersey: Prentice Hall, 1990.

[30] Merletti, R., Conte, L., and C. Orzio. "Indices of Muscle Fatigue." *J. Electromyographic Kinesiology* 1 (1991): 20-33.

[31] Merletti, R., and S. Roy. "Myoelectric and Mechanical Manifestations of Muscle Fatigue in Voluntary Contractions." *J. Orthopedic Sports Physical Therapy* 24 (1996): 342-53.

[32] Chapa, J., and R. Rao. "Algorithms for Designing Wavelets to Match a Specified Signal." *IEEE Trans. on Signal Processing* 48:12 (2000): 3395-3406.